BRAINLAB

IMAGING EVOLUTO E PRECISIONE IN RADIOCHIRURGIA CEREBRALE

ING.PIER PAOLO RAGUZZI
SALES MANAGER RT
BRAINLAB ITALIA SRL

BRAINLAB - CORPORATE OVERVIEW

- Founded in Munich, Germany in 1989
- Privately held since inception
- Over 1300 employees in 17 offices worldwide
- More than 290 R&D engineers
- More than 5,000 systems installed

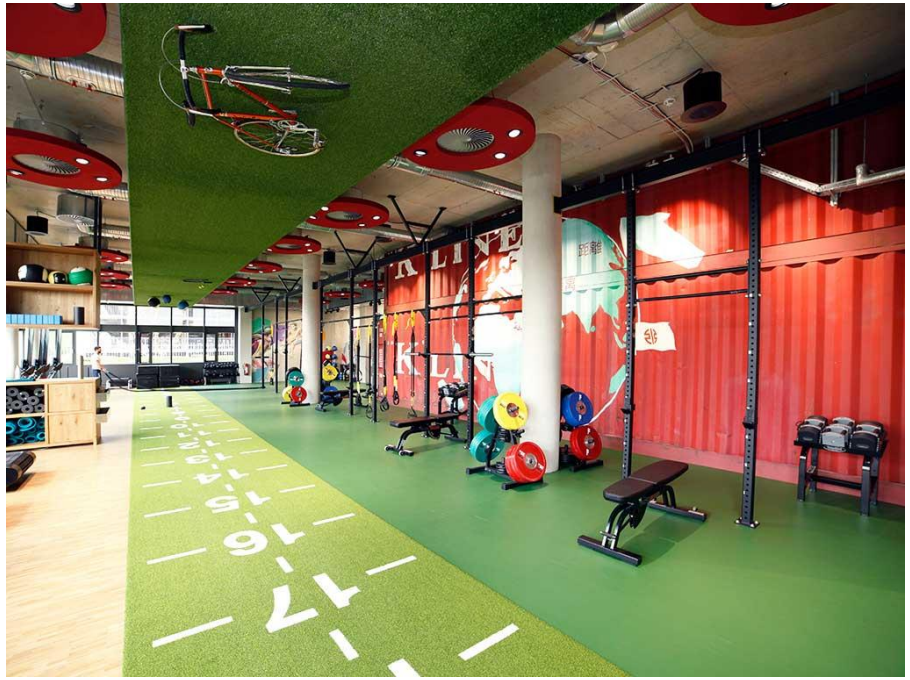

RadioChirurgia Stereotassica Brain

Meningiomas of the anterior skull base

Optic neuropathy

Traditional limits

Doses < 8 Gy

Tumour - AOP distance > 3mm

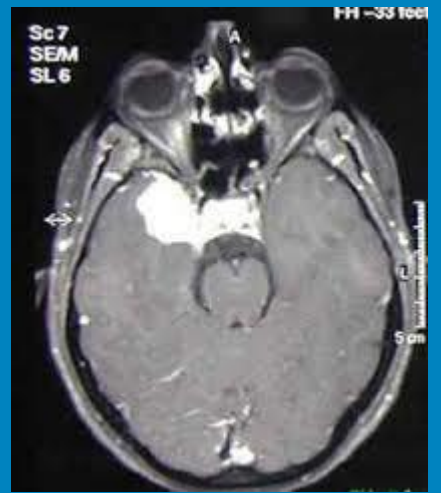

Stafford SL et al. A study on the radiation tolerance of the optic nerves and chiasm after stereotactic radiosurgery. *Int J Radiat Oncol Biol Phys* 2003

Tishler RB et al. Tolerance of cranial nerves of the cavernous sinus to radiosurgery. *Int J Radiat Oncol Biol Phys* 1993

Curtesy of

Fondazione I.R.C.C.S. Istituto Neurologico Carlo Besta

Sistema Socio Sanitario Regione Lombardia

Perioptic Meningiomas

single-session Radiosurgery

Hasegawa T et al. 2010 Tolerance of the optic apparatus in single-fraction irradiation using stereotactic radiosurgery: Evaluation in 100 patients with craniopharyngioma.

14 Gy

Leavitt JA et al. 2013 Long-term evaluation of radiation-induced optic neuropathy after single-fraction stereotactic radiosurgery

12 Gy

Pollock BE et al. 2014 Dose-Volume Analysis of Radiation-Induced Optic Neuropathy After Single-Fraction Stereotactic Radiosurgery

12 Gy

Curtesy of

Sistema Socio Sanitario

Fondazione I.R.C.C.S. Istituto Neurologico Carlo Besta

Regione Lombardia

Perioptic Meningiomas
multisession Radiosurgery

Multisession radiosurgery for optic nerve sheath meningiomas, an effective option: preliminary results of a single-center experience
Marchetti M, Bianchi S, Milanesi I, Bergantin A, Bianchi L, Broggi G, Fariselli L.
Neurosurgery. 2011

25Gy/5fr

Staged image guided robotic radiosurgery for optic nerve sheath meningiomas. Romanelli P, Bianchi L, Muacevic A, Beltramo G.
Comput Aided Surg. 2011

20Gy/4fr

Diagnosis and management of optic nerve sheath meningiomas
Shapey J, Sabin HI, Danesh-Meyer HV, Kaye AH
J Clin Neurosci. 2013

20Gy/4fr

Curtesy of

Sistema Socio Sanitario
Fondazione I.R.C.C.S. Istituto Neurologico Carlo Besta
Regione Lombardia

Fig. 1: RMN di un paziente con Meningingioma

BRAINLAB ELEMENTS

Concept

- Moduli software per obbiettivi clinici specifici
- Vantaggio della **modularita´** al fine di costruire e customizzare i vari workflow
- **Algoritmi intelligenti** e ambiente utente intuitivo
- Al Servizio di piu´specialita´cliniche dalla **Radioterapia alla Neurochirurgia**

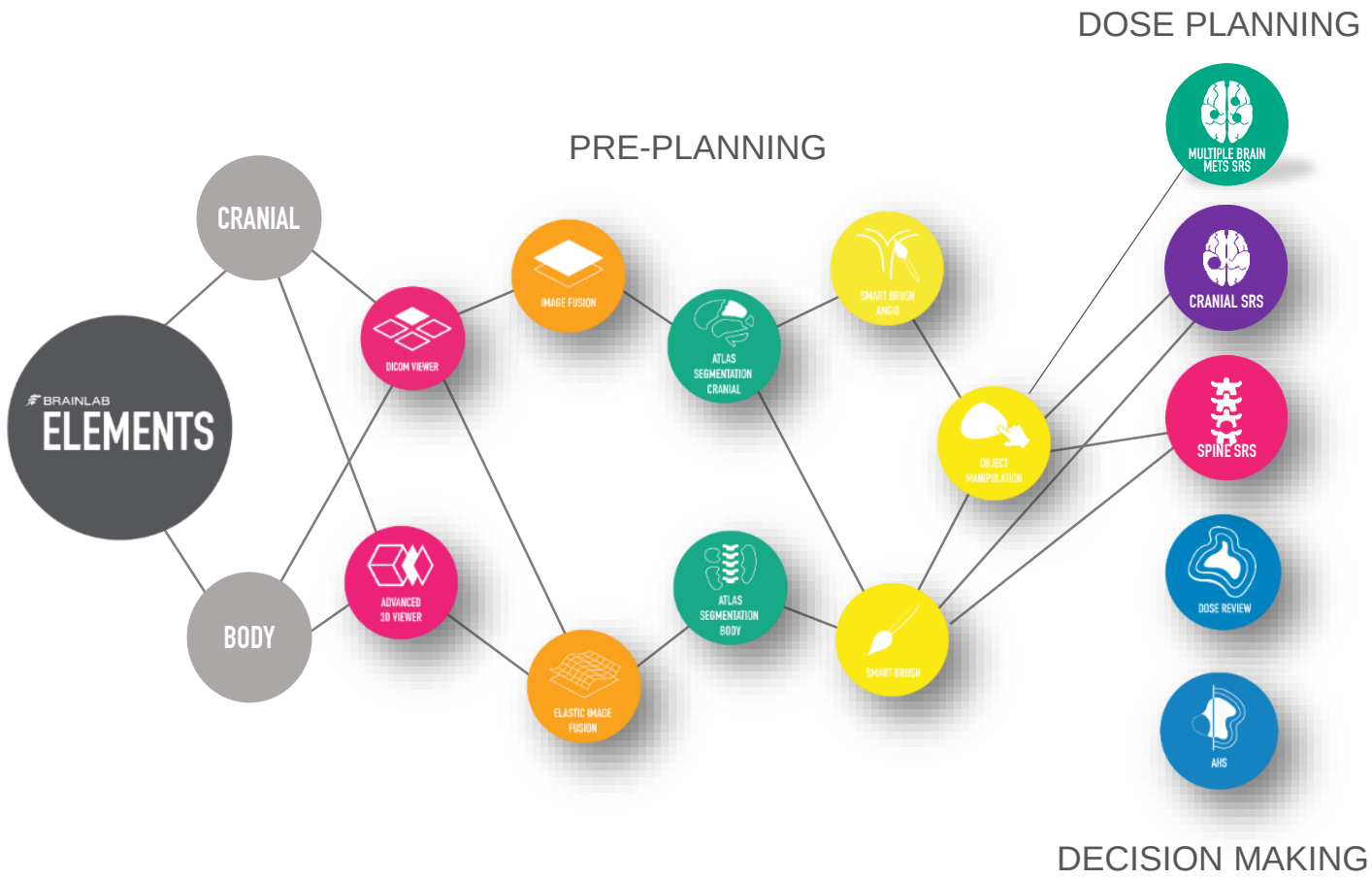

BRAINLAB ELEMENTS

Software per indicazioni specifiche

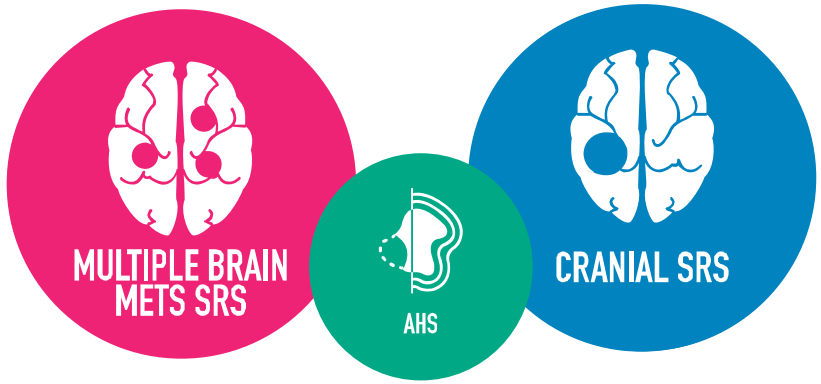

Brain Metastases

Cranial Tumors

Spine Metastases

Functional Indications

Vascular Malformations

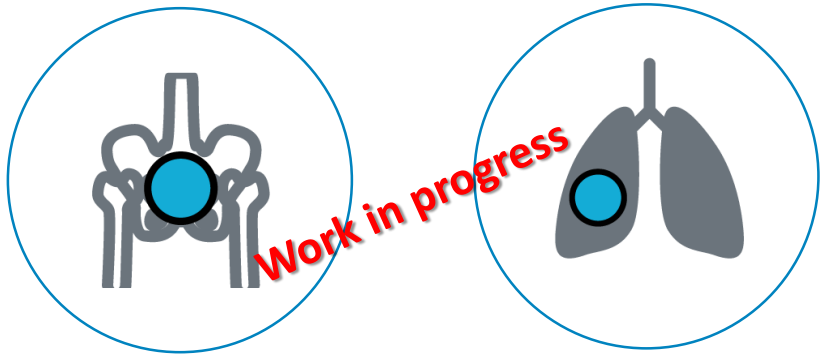

Prostate

Lung

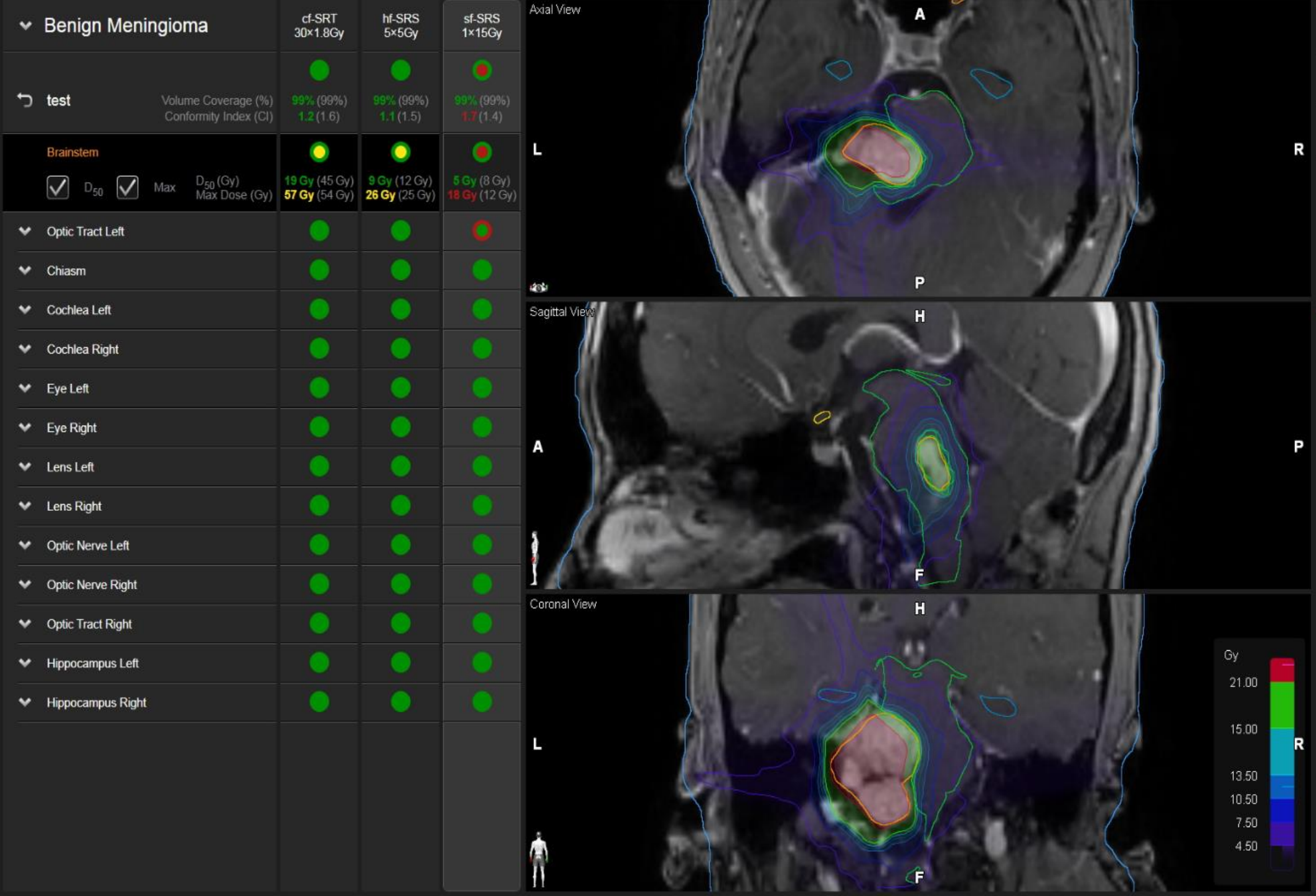
Benign Meningioma
cf-SRT 30×1.8Gy
hf-SRS 5×5Gy
sf-SRS 1×15Gy
test
Volume Coverage (%) 99% (99%) 99% (99%) 99% (99%)
Conformity Index (CI) 1.2 (1.6) 1.1 (1.5) 1.7 (1.4)
Brainstem
D50 Max D50 (Gy) Max Dose (Gy)
19 Gy (45 Gy) 57 Gy (54 Gy)
9 Gy (12 Gy) 26 Gy (25 Gy)
5 Gy (8 Gy) 18 Gy (12 Gy)
Optic Tract Left
Chiasm
Cochlea Left
Cochlea Right
Eye Left
Eye Right
Lens Left
Lens Right
Optic Nerve Left
Optic Nerve Right
Optic Tract Right
Hippocampus Left
Hippocampus Right
Axial View
Sagittal View
Coronal View
A
P
L
R
H
F
Gy
21.00
15.00
13.50
10.50
7.50
4.50
DEMO, Large benign acou... AHSA 02-2014/08
Adaptive Hybrid Surgery Analysis
Scroll
Zoom
Pan
Windowing
Dose
Dose Off
Dose Distribution
Highlight 4.50 Gy
Back
Done
BRAINLAB

BRAINLAB

BRAINLAB ELEMENTS

ANATOMICAL MAPPING

UNIVERSAL SOFTWARE MODEL

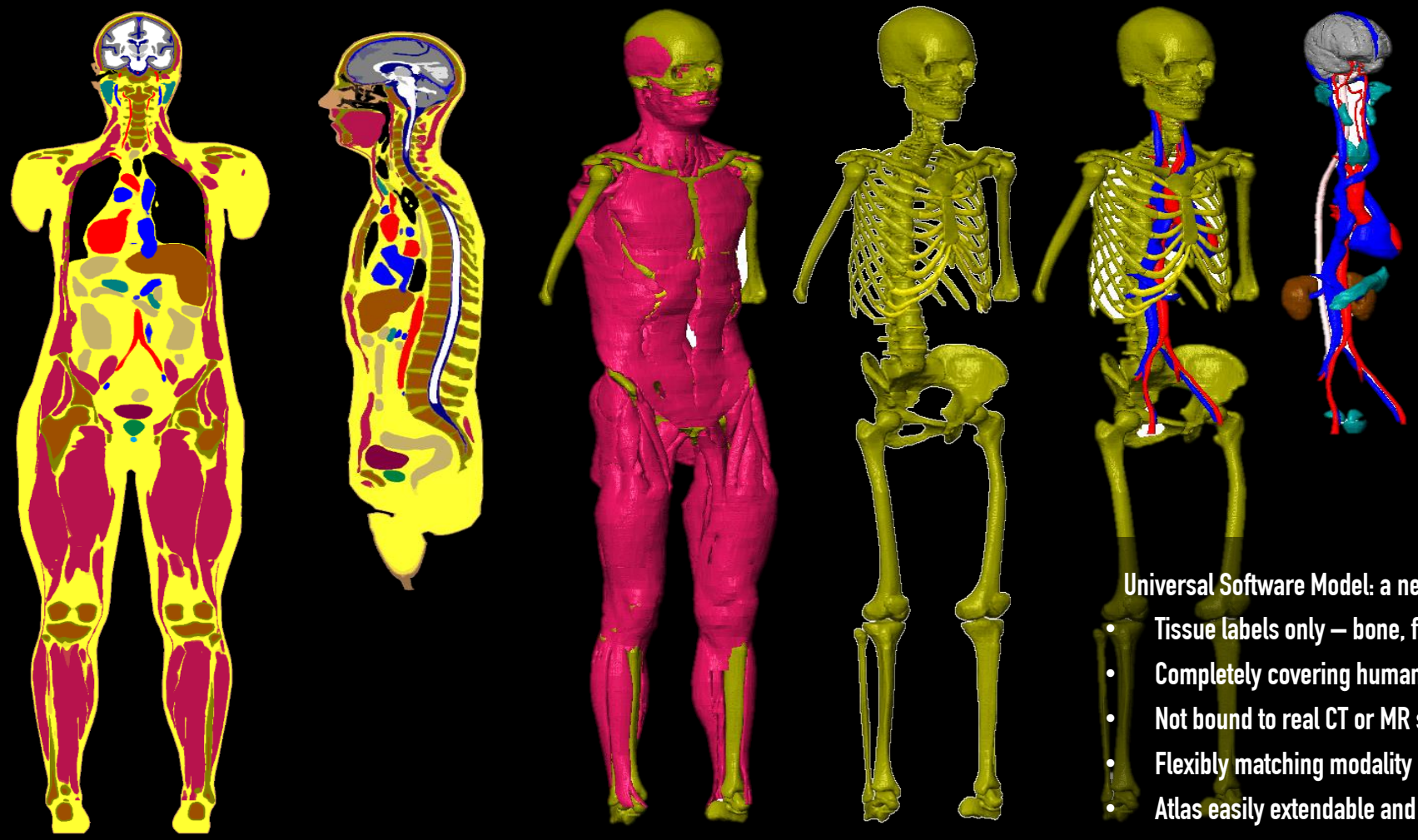

Universal Software Model: a new segmentation approach

- Tissue labels only – bone, fat, muscles, organs
- Completely covering human body, not just critical structures
- Not bound to real CT or MR scans
- Flexibly matching modality diversity
- Atlas easily extendable and refinable
- Better & more robust registrations

BRAINLAB

UNIVERSAL SOFTWARE MODEL

Elements Segmentation Cranial	Elements Segmentation H&N	Elements Segmentation Thoracic	Elements Segmentation Spine	Elements Segmentation Pelvic
Planned validated structures (MR)	**Planned validated structures (CT)**	**Planned validated structures (CT)**	**Planned validated structures (CT)**	**Planned validated structures (CT)**
Brainstem	Brainstem	Aorta	Spinal Canal	Prostate
Optic Nerve	Cricoid Cartilage	Vena Cava Inferior	Spinal Cord	Bladder
Chiasm	Hyoid	Clavicle	Vertebra C01	Rectum
Optic Tract	Cochlea	Heart	Vertebra C02	Hip Joint
Eyes	Eye	Kidney	Vertebra C03	Seminal Vesicle
Lens	Lens	Lung	Vertebra C04	Penile Bulb
Whole Brain	Lymph Level 1A	Liver	Vertebra C05	
Cochlea	Lymph Level 1B	Esophagus	Vertebra C06	
Hippocampus	Lymph Level 2	Ribs	Vertebra C07	
Cerebellum	Lymph Level 3	Sternum	Vertebra T01	
Temporal Lobe	Lymph Level 4	Manubrium		
Cerebrum	Lymph Level 5	Trachea		
White Matter	Lymph Level 6			
Gray Matter	Lymph Node RCL			
Hypothalamus	Lymph Node RP			
Putamen	Lymph Node RST			
Corpus Callosum	Parotid Gland			
Pineal Gland	Sternocleidomastoid Muscle			
CSF	Submandibular Gland			
Brain	Mandible			
Caudatus	Thyroid Cartilage			
Ventricles	Thyroid Gland			
Geniculate Body				
Globus Pallidus				
Pituitary Gland				
Nucleus Caudatus				
Capsula Externa				
Capsula Interna				
Amygdala				
Thalamus				

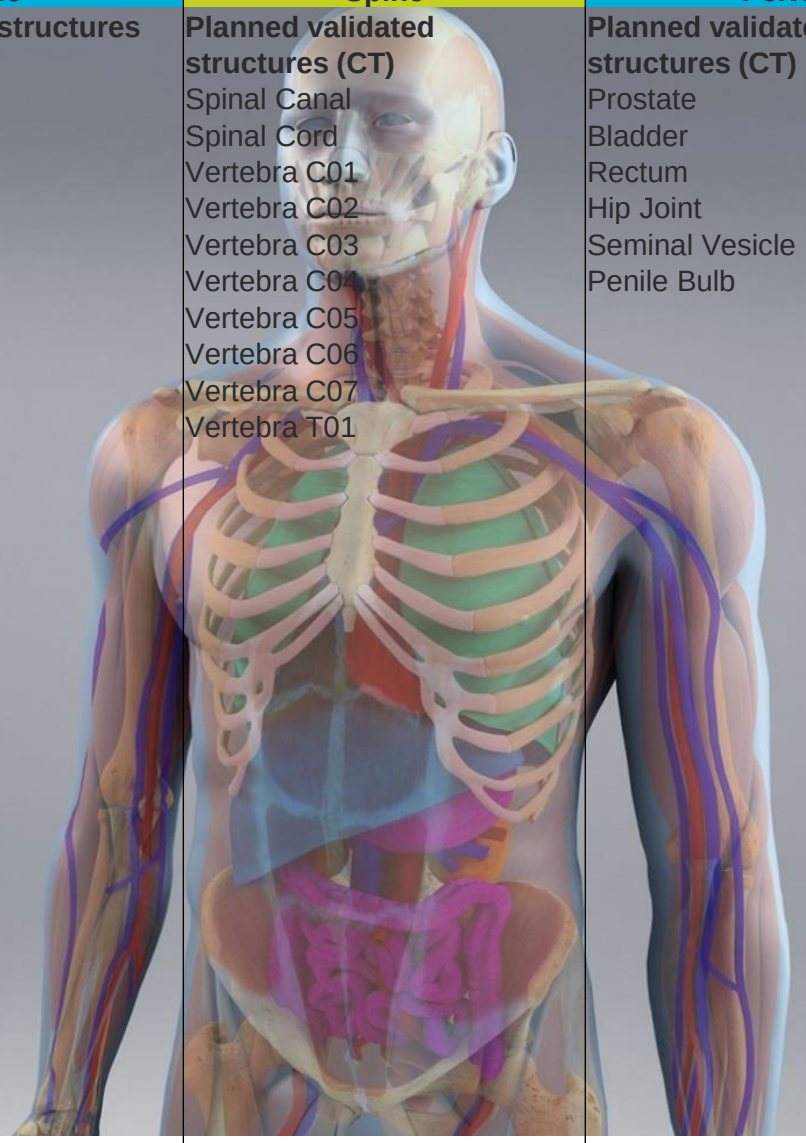

ANATOMICAL MAPPING

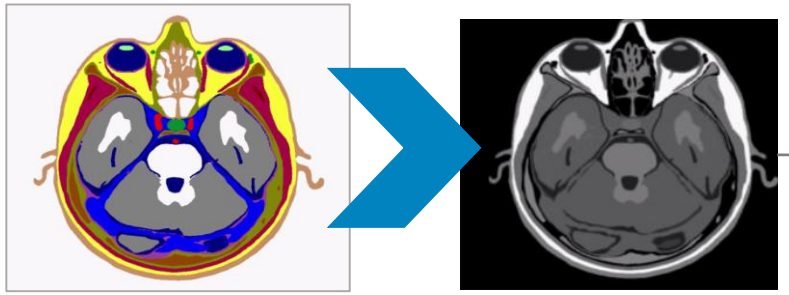

Simulation of atlas – mimicing patient scan

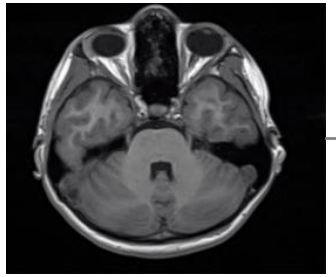

Actual patient scan

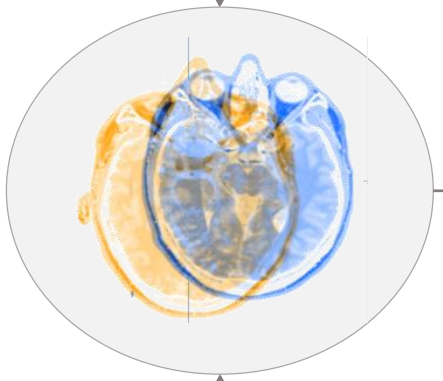

Deformable
Co-registration

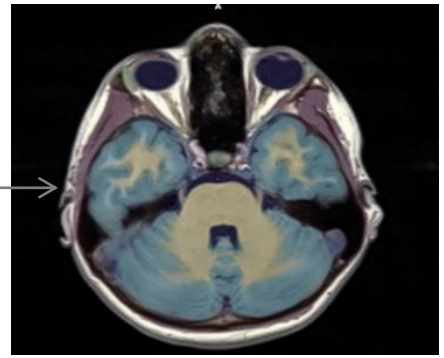

Complete tissue labeling

ANATOMICAL MAPPING

- Basato su un modello tissutale universale completamente nuovo
- Adattabile dinamicamente e indipendente dalla modalita´di acquisizione
- Classificazione completa del tessuto in tutto il corpo
- Vengono considerate sequenze MR multiple di uno studio per eseguire la registrazione
- Visualizzazione completa della registrazione sottostante

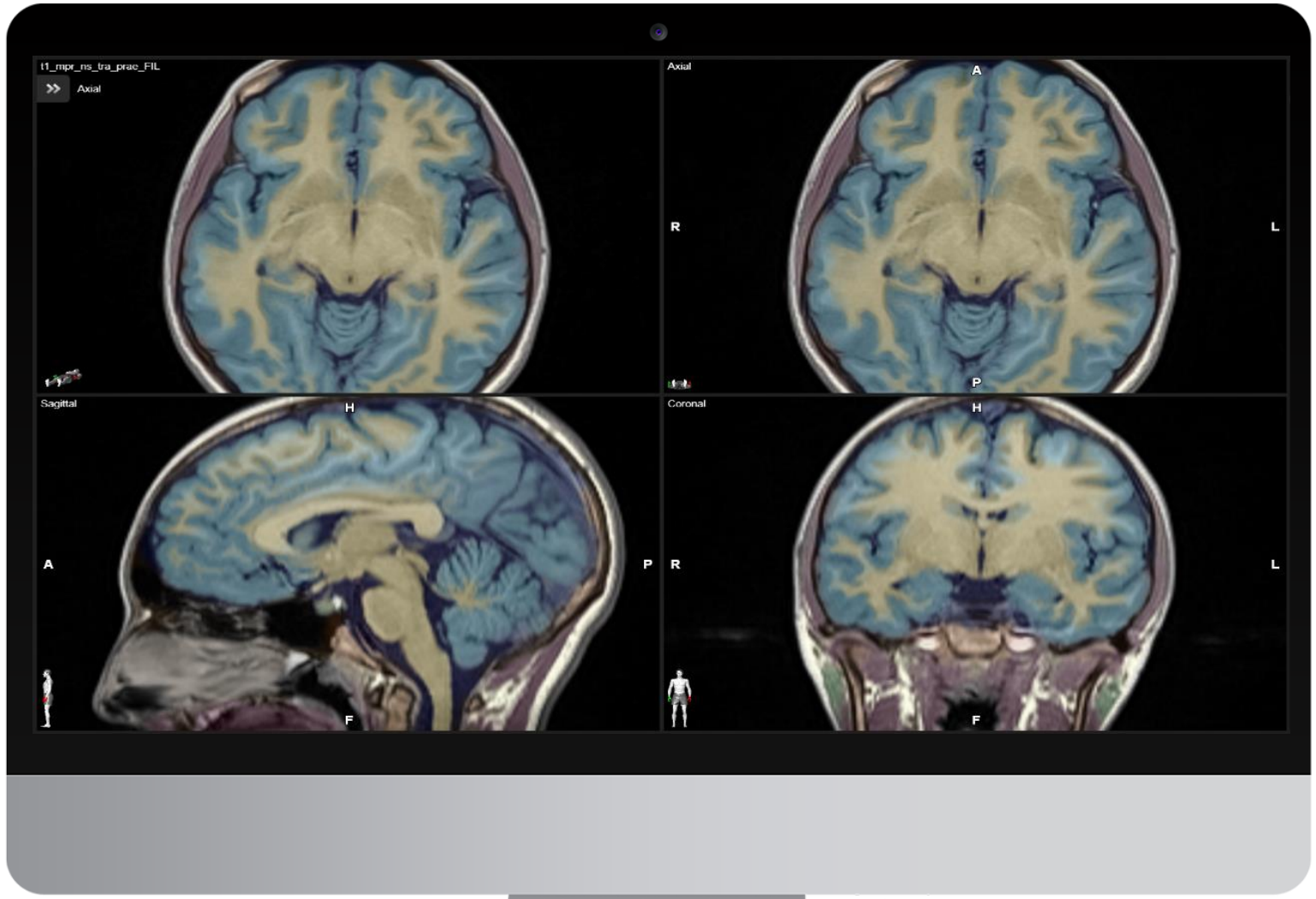

ANATOMICAL MAPPING

- Basato su un modello tissutale universale completamente nuovo
- Adattabile dinamicamente e indipendente dalla modalita´di acquisizione
- Classificazione completa del tessuto in tutto il corpo
- Vengono considerate sequenze MR multiple di uno studio per eseguire la registrazione
- Visualizzazione completa della registrazione sottostante

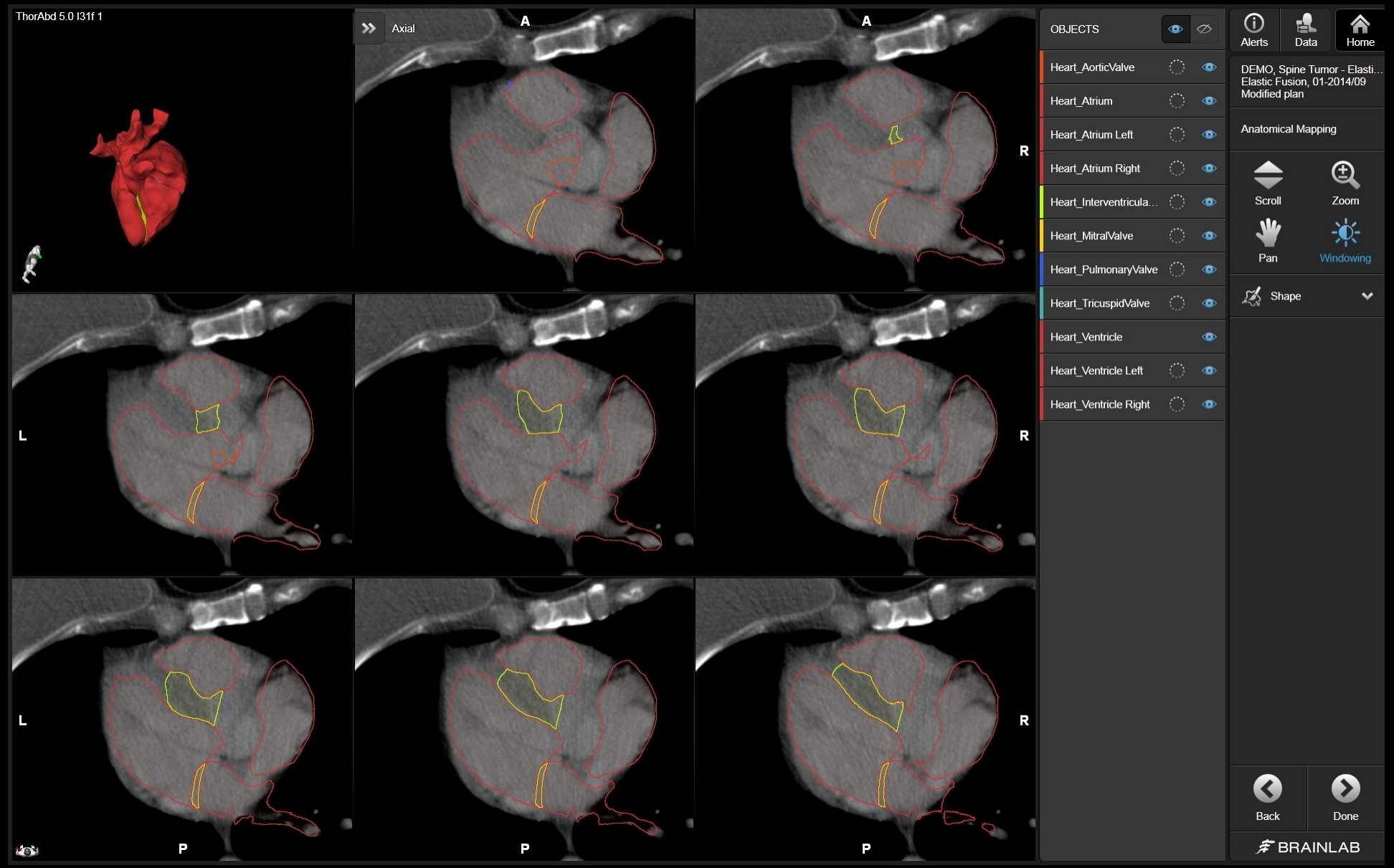

Courtesy of University of Torino – RT dep. Prof. U.Ricardi

BRAINLAB

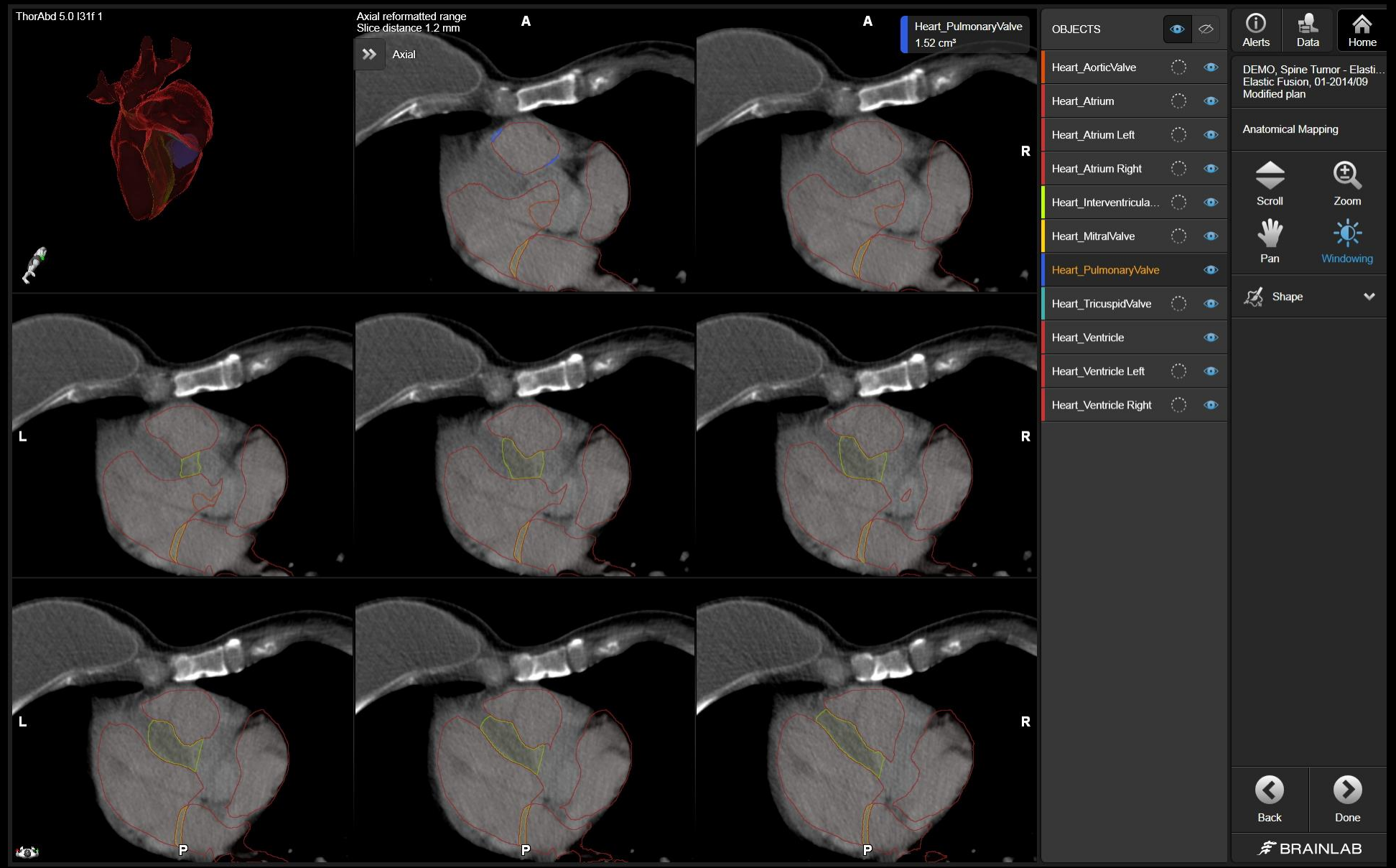

Courtesy of University of Torino – RT dep. Prof. U.Ricardi

BRAINLAB

BRAINLAB

BRAINLAB ELEMENTS

IMAGE FUSION

- CRANIAL DISTORTION CORRECTION

- SPINE CURVATURE CORRECTION

CRANIAL DISTORTION CORRECTION

IMAGE FUSION con CRANIAL DISTORTION CORRECTION

- Co-registrazione multi-modale deformabile: Cranial MR ←→ planning CT
- Permette il contornamento del tumore basato su MR utilizzando il data set corretto con dalla distorsione.
- Nessuna necessita´di operare una fusion locale con ROI

QUALITY ASSURANCE

- Valutazioni della posizione e grandezza delle distorsioni
- Panoramica rapida su quale MR è la scelta migliore per la definizione precisa del bersaglio
- Facile confronto dei risultati corretti rispetto alla versione rigida o distorta.

CRANIAL DISTORTION CORRECTION

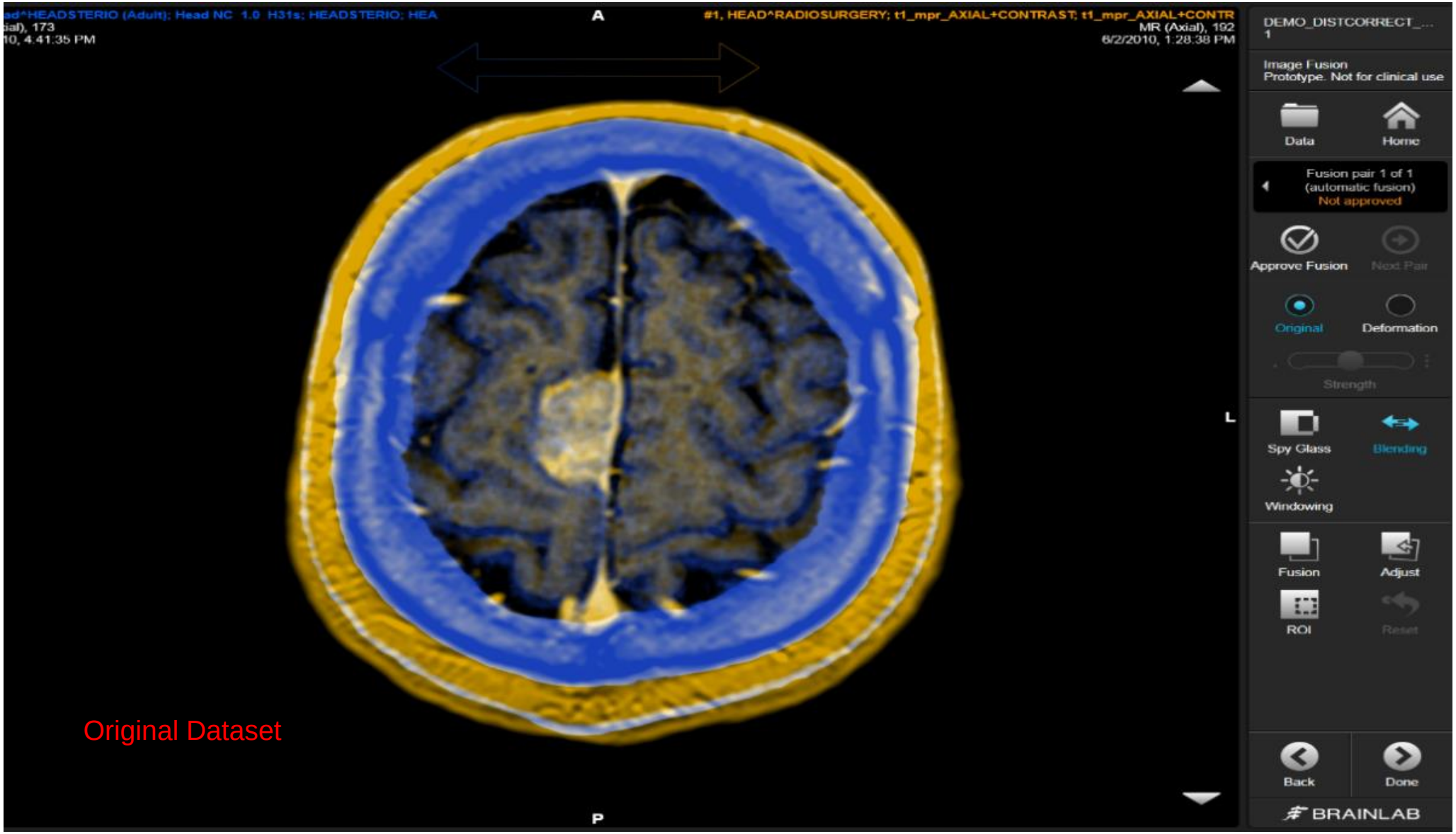

CRANIAL DISTORTION CORRECTION

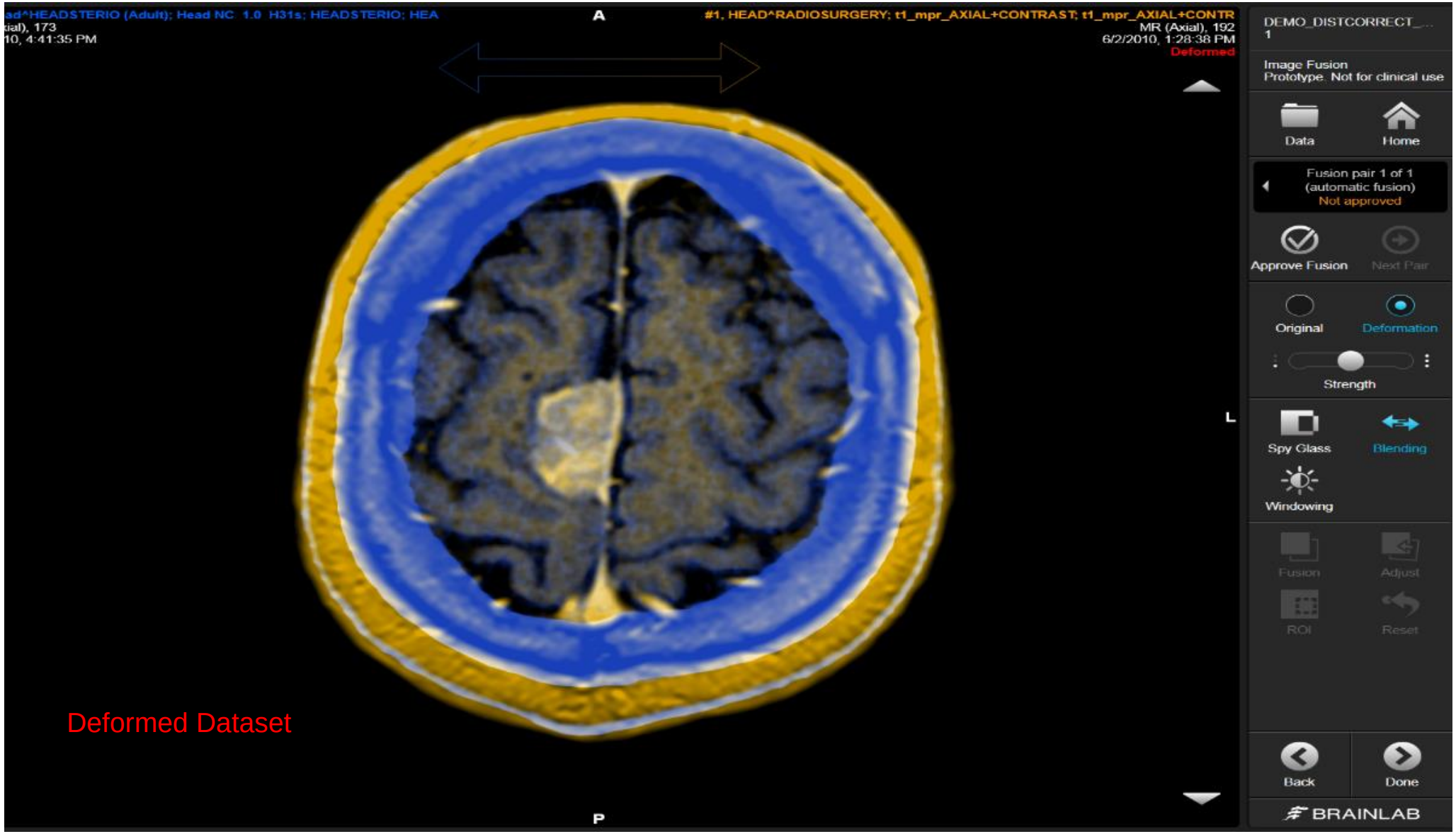

CRANIAL DISTORTION CORRECTION

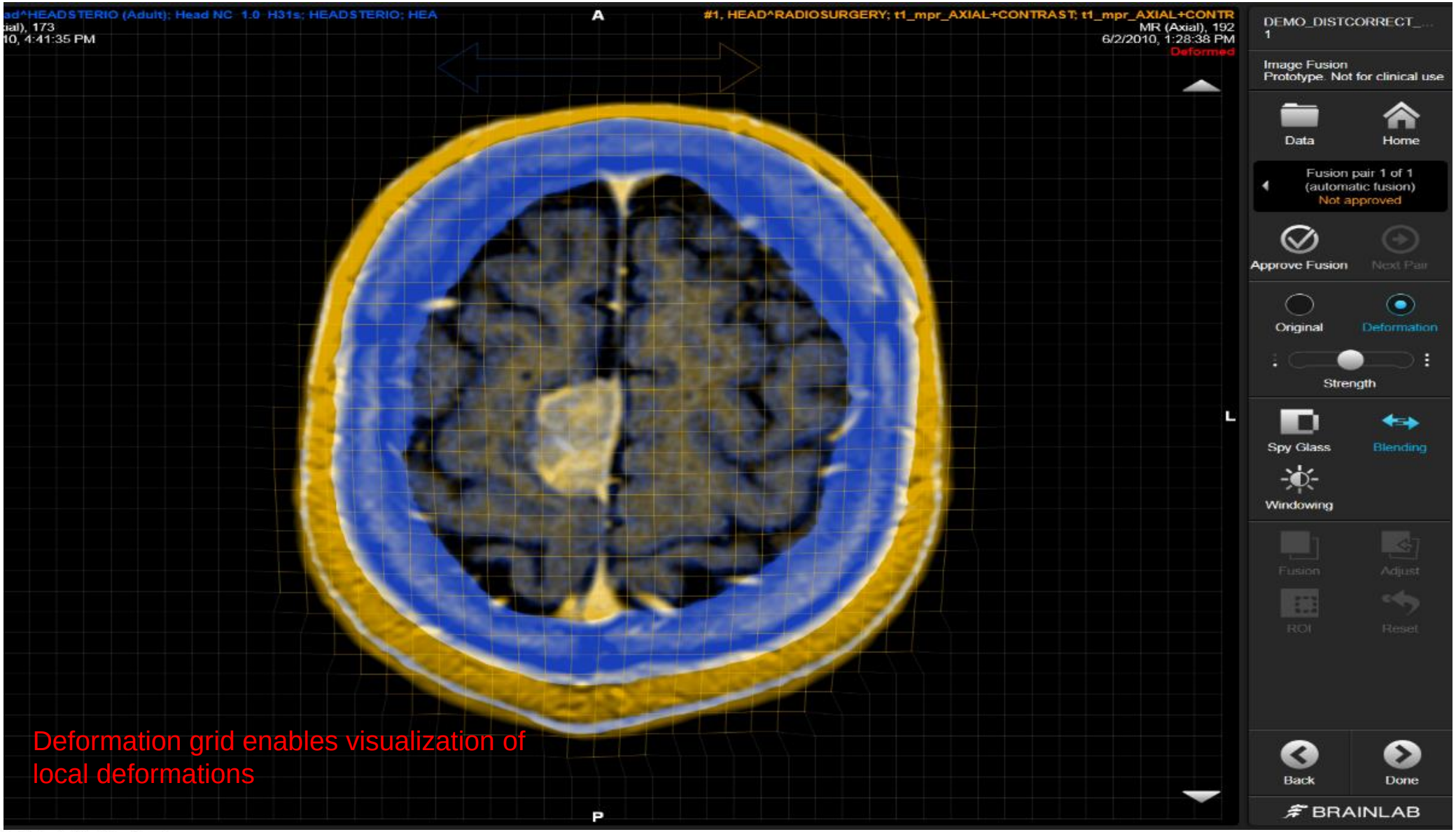

Deformation grid enables visualization of local deformations

Kim, J. et al. Image-guided localization accuracy of stereoscopic planar and volumetric imaging methods for stereotactic radiation surgery and stereotactic body radiation therapy: a phantom study. Int. J. Radiat. Oncol. Biol. Phys. 79, 1588–96 (2011).

EXACTRAC POSITIONING ACCURACY FOR MULTIPLE TARGETS IN INTRACRANIAL IMAGE-GUIDED RADIATION THERAPY: A PHANTOM STUDY

DEDICATED PHANTOM
The phantom is positioned with ExacTrac and the positioning is evaluated with CBCT. The effect of rotations as a function of distance from the isocenter is investigated by introducing roll and pitch and evaluating the introduced shift for each of the nine targets

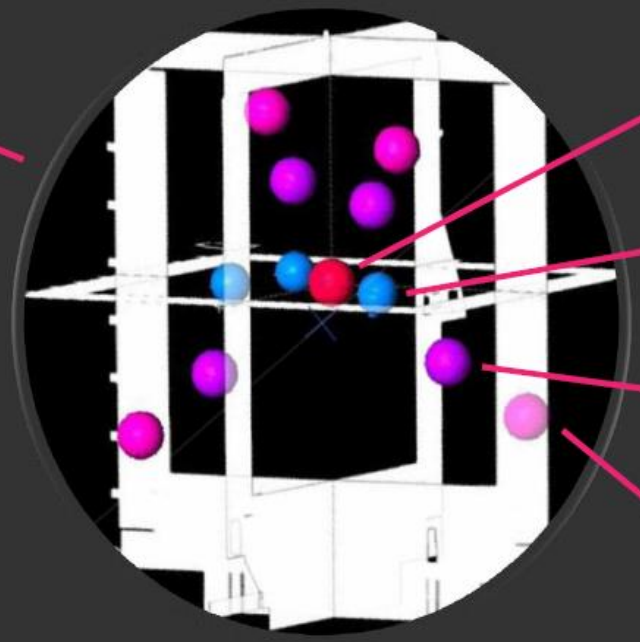

ONE TARGET at isocenter
(reference target)

THREE SPHERES
(for image-guided marker fusion)

FOUR TARGETS at 52 mm
(covered by 2.5 mm leafs)

FOUR TARGETS at 87 mm
(covered by 5 mm leafs)

A Japanese group build a dedicated phantom with nine spherical metastases to reveal the dramatic effects of uncompensating rotations when treating multiple targets with a single isocenter. They further demonstrate how ExacTrac is able to compensate for these potential errors and realize submillimeter accuracy for all targets

3D VECTOR POSITIONING ERRORS FOR EACH TARGET AS A FUNCTION OF ROTATION AND REMAINING ERROR AFTER EXACTRAC CORRECTION

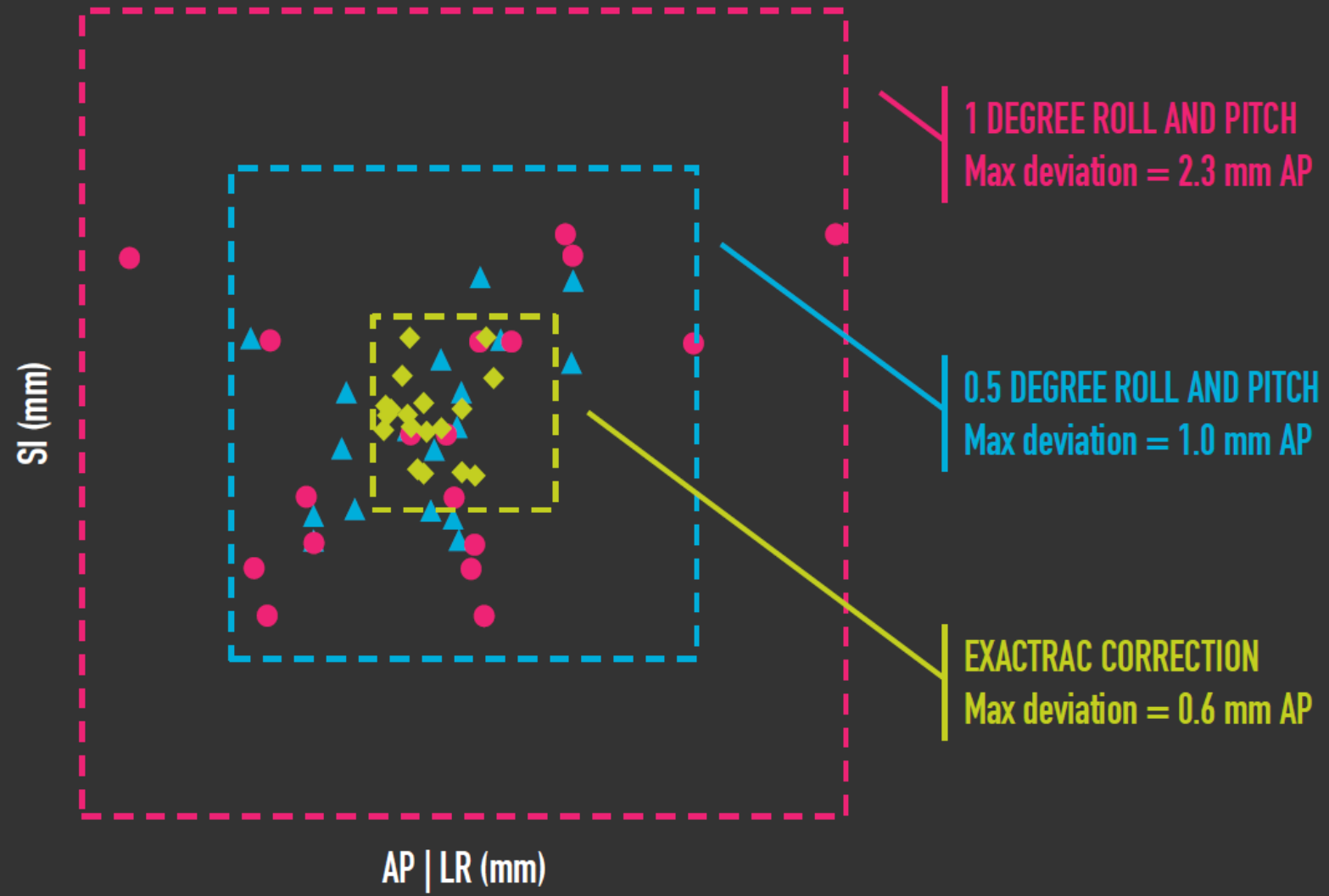

SPINAL CURVATURE CORRECTION

IMAGE FUSION con CRANIAL DISTORTION CORRECTION

- Co-registrazione multi-modale deformabile: Cranial MR ←→ planning CT
- Permette il contornamento del tumore basato su MR utilizzando il data set corretto con dalla distorsione.
- Nessuna necessita´di operare una fusion locale con ROI

QUALITY ASSURANCE

- Valutazioni della posizione e grandezza delle distorsioni
- Panoramica rapida su quale MR è la scelta migliore per la definizione precisa del bersaglio
- Facile confronto dei risultati corretti rispetto alla versione rigida o distorta.

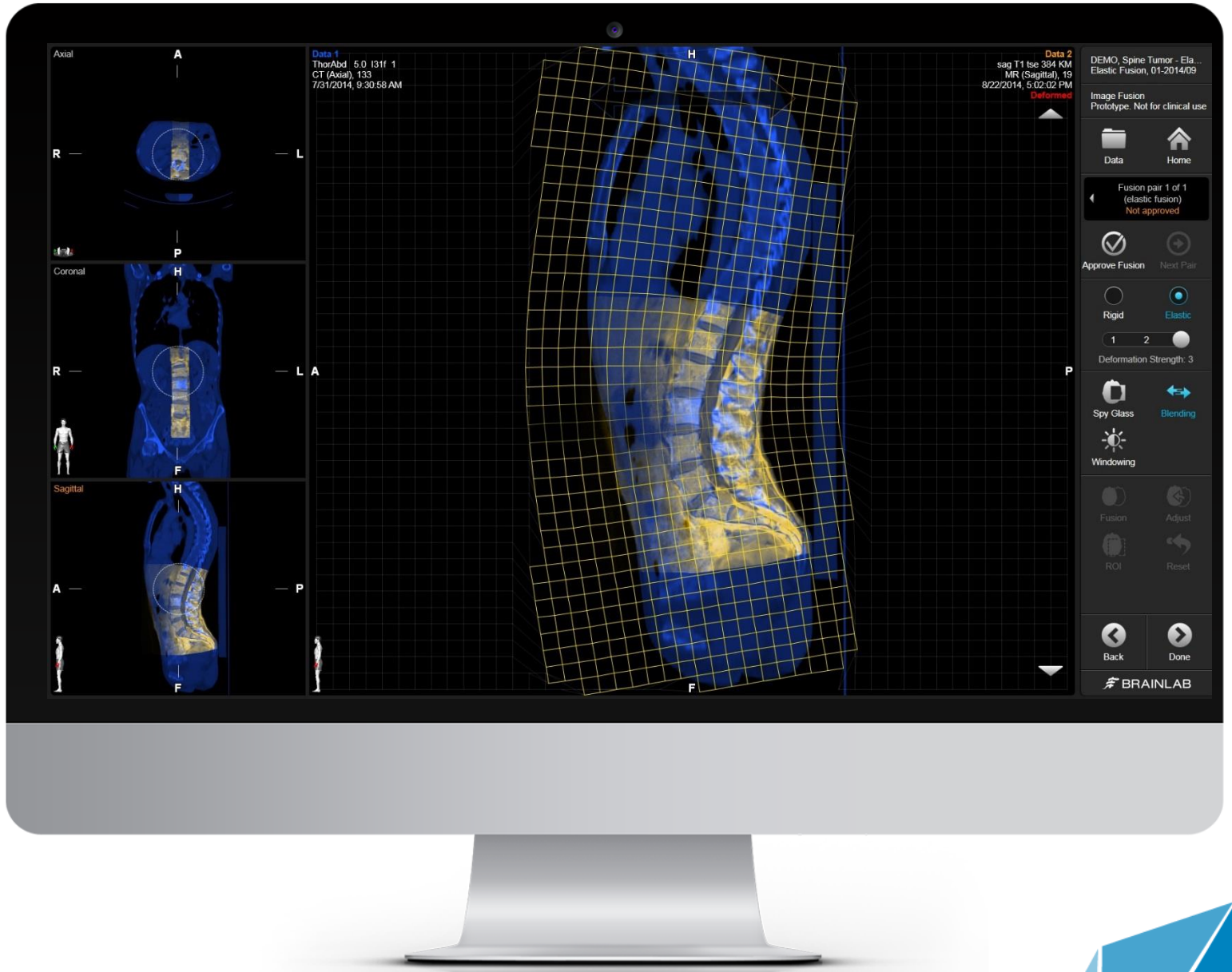

SPINAL CURVATURE CORRECTION

IMAGE FUSION con CRANIAL DISTORTION CORRECTION

- Co-registrazione multi-modale deformabile: Cranial MR ←→ planning CT
- Permette il contornamento del tumore basato su MR utilizzando il data set corretto con dalla distorsione.
- Nessuna necessita´di operare una fusion locale con ROI

QUALITY ASSURANCE

- Valutazioni della posizione e grandezza delle distorsioni
- Panoramica rapida su quale MR è la scelta migliore per la definizione precisa del bersaglio
- Facile confronto dei risultati corretti rispetto alla versione rigida o distorta.

SPINAL CURVATURE CORRECTION

IMAGE FUSION con CRANIAL DISTORTION CORRECTION

- Co-registrazione multi-modale deformabile: Cranial MR ←→ planning CT
- Permette il contornamento del tumore basato su MR utilizzando il data set corretto con dalla distorsione.
- Nessuna necessita´di operare una fusion locale con ROI

QUALITY ASSURANCE

- Valutazioni della posizione e grandezza delle distorsioni
- Panoramica rapida su quale MR è la scelta migliore per la definizione precisa del bersaglio
- Facile confronto dei risultati corretti rispetto alla versione rigida o distorta.

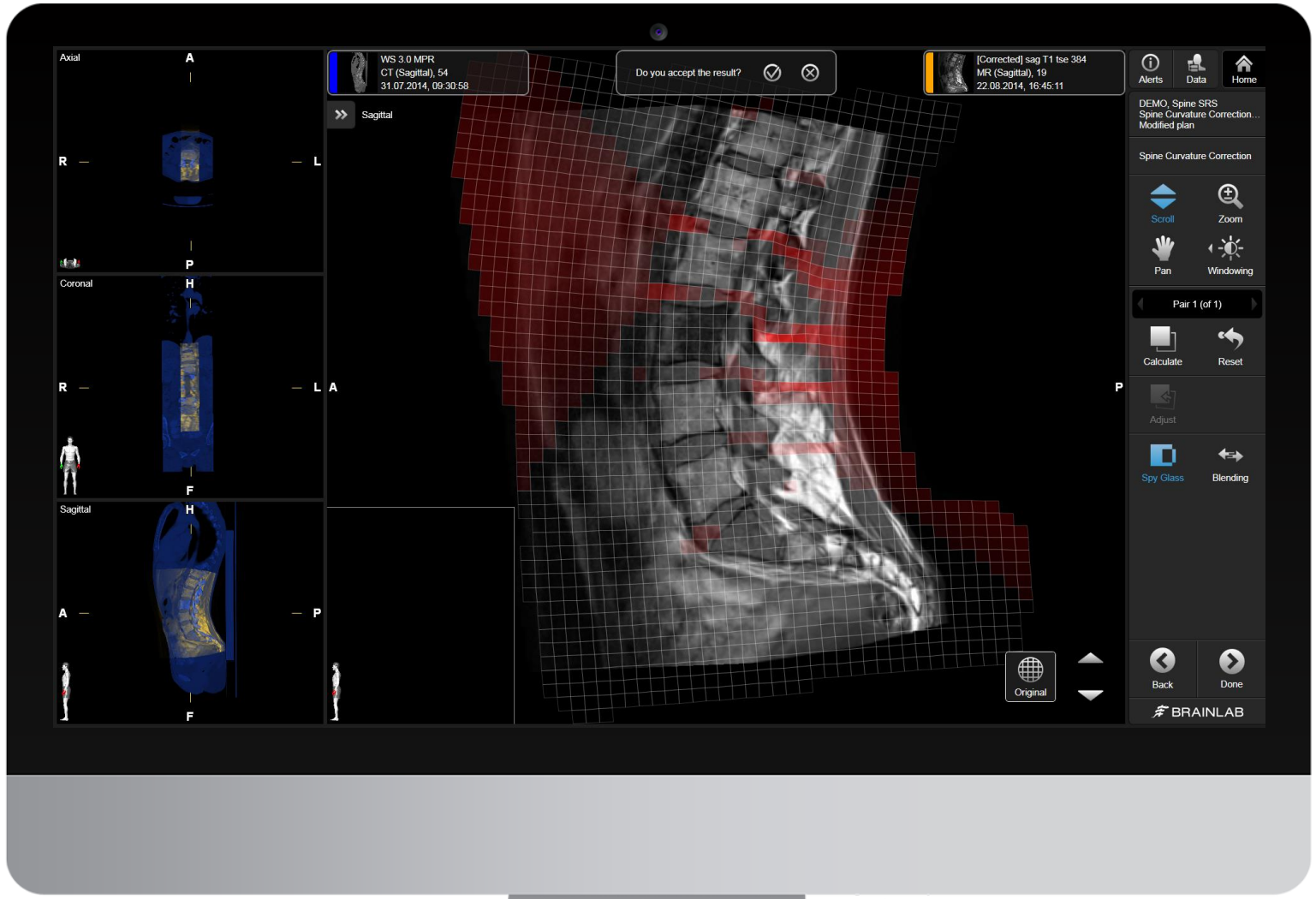

SPINE SRS ELEMENT

SPINE SMARTBRUSH

- Funzionalita´di contornamento multimodale: due data sets sono utilizzati simultaneamente.
- Segmentazione automatica della vertebra
- Vista specifica per Spine per contornamento con SmartBrush
- Selezione della vertebra di interesse in 3D. Zoom automatico e focalizzato in viste 2D.

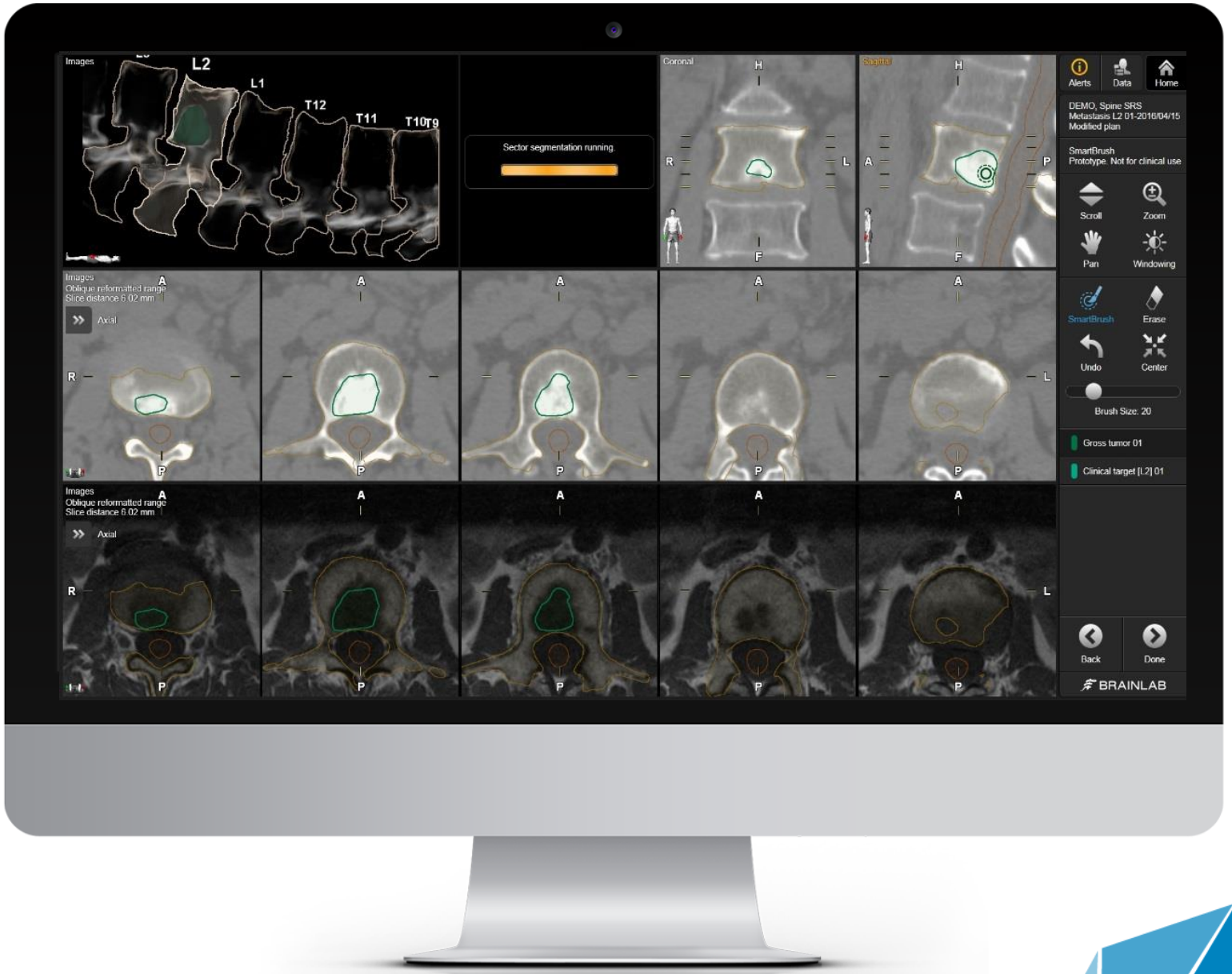

SPINE SRS ELEMENT

CME ASTRO

International Journal of Radiation Oncology biology • physics
www.redjournal.org

Clinical Investigation: Central Nervous System Tumor

International Spine Radiosurgery Consortium Consensus Guidelines for Target Volume Definition in Spinal Stereotactic Radiosurgery

Brett W. Cox, MD,[*,1] Daniel E. Spratt, MD,[*,1] Michael Lovelock, PhD,[†] Mark H. Bilsky, MD,[‡] Eric Lis, MD,[§] Samuel Ryu, MD,[‖] Jason Sheehan, MD,[¶] Peter C. Gerszten, MD, MPH,[**] Eric Chang, MD,[††] Iris Gibbs, MD,[‡‡] Scott Soltys, MD,[‡‡] Arjun Sahgal, MD,[§§] Joe Deasy, PhD,[†] John Flickinger, MD,[‖‖] Mubina Quader, PhD,[‖‖] Stefan Mindea, MD,[¶¶] and Yoshiya Yamada, MD[‡‡]

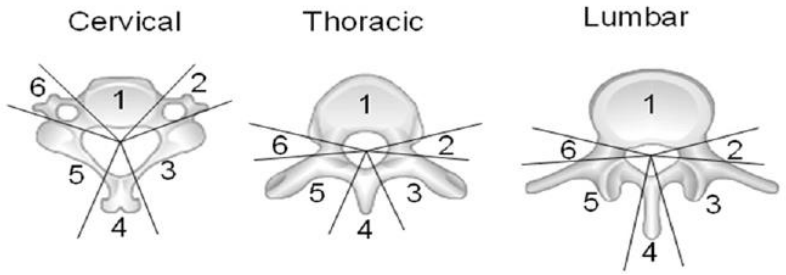

BRAINLAB

BRAINLAB ELEMENTS

SMARTBRUSH ANGIO

TRADITIONAL WORKFLOW USING LOCALIZER

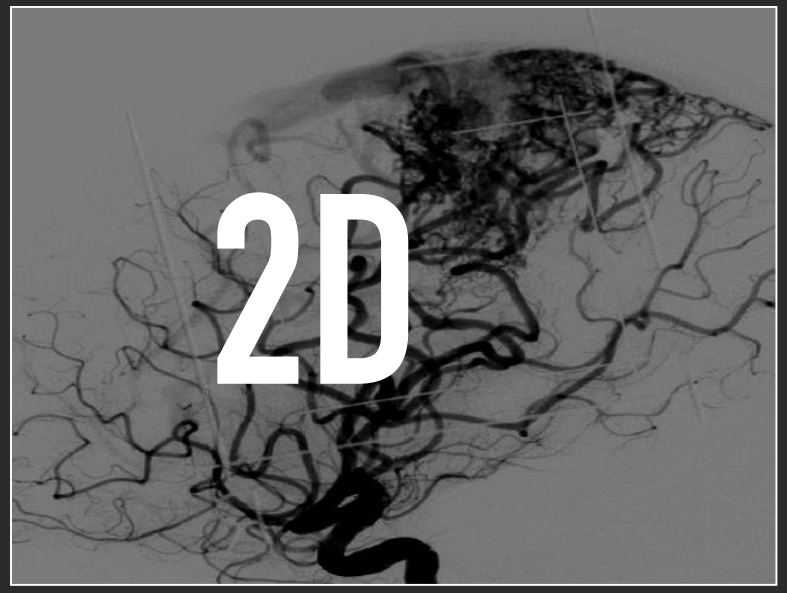

MUTUAL
LOCALIZATION

INVASIVE HEAD FRAME
REPEATED
ANGIOGRAPHY

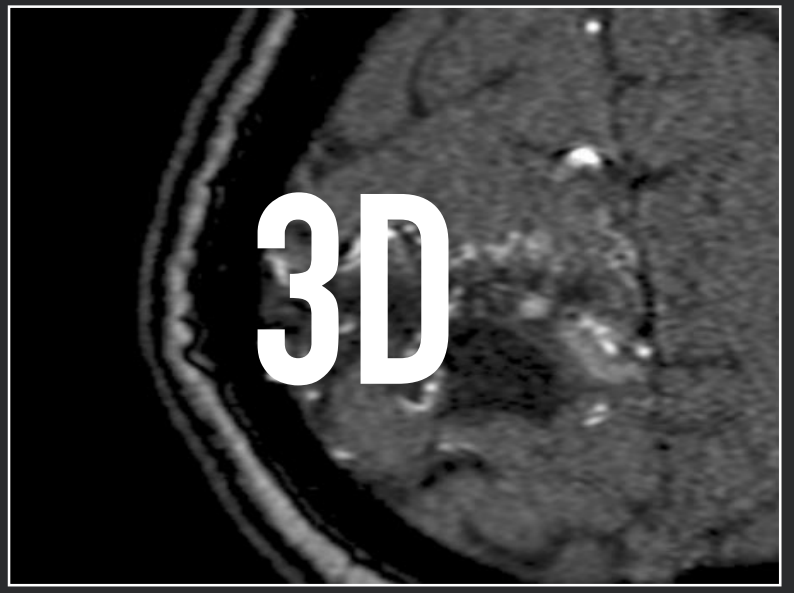

SMARTBRUSH ANGIO WORKFLOW

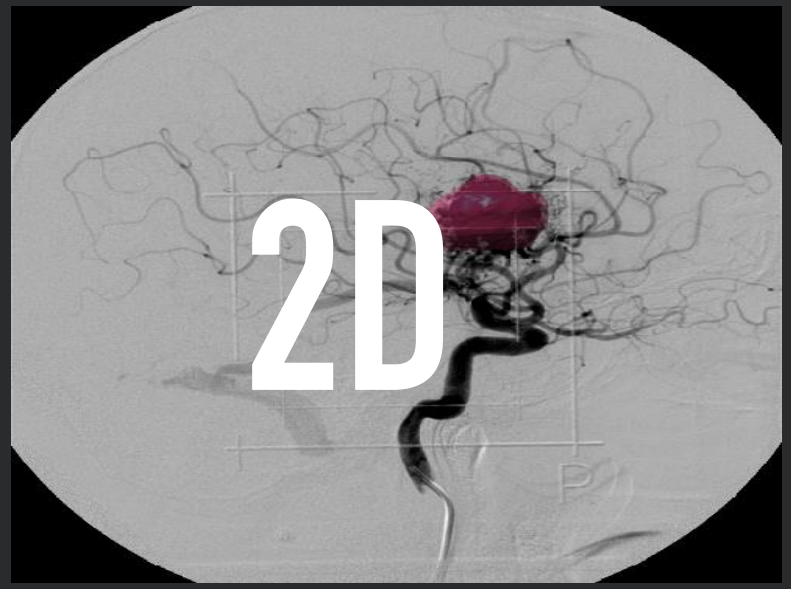

VESSEL TREE
FUSION

SMART BRUSH
ANGIO

FRAMELESS MASK
NO ADDITIONAL
ANGIOGRAPHY

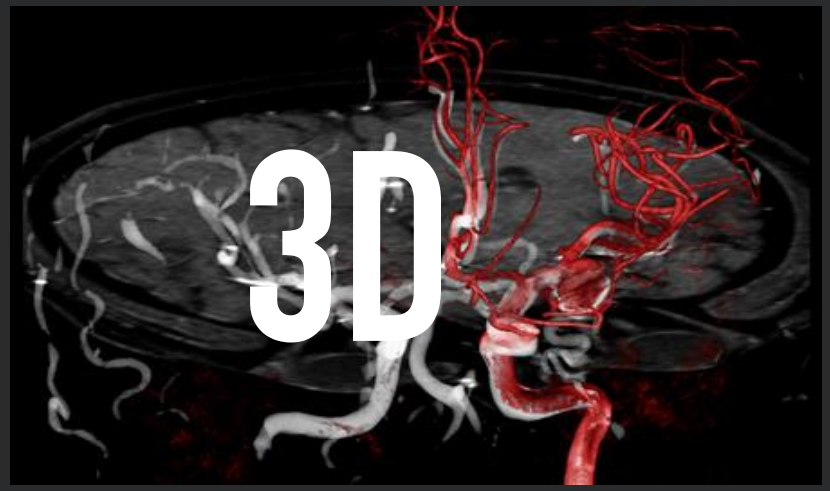

SMARTBRUSH ANGIO WORKFLOW

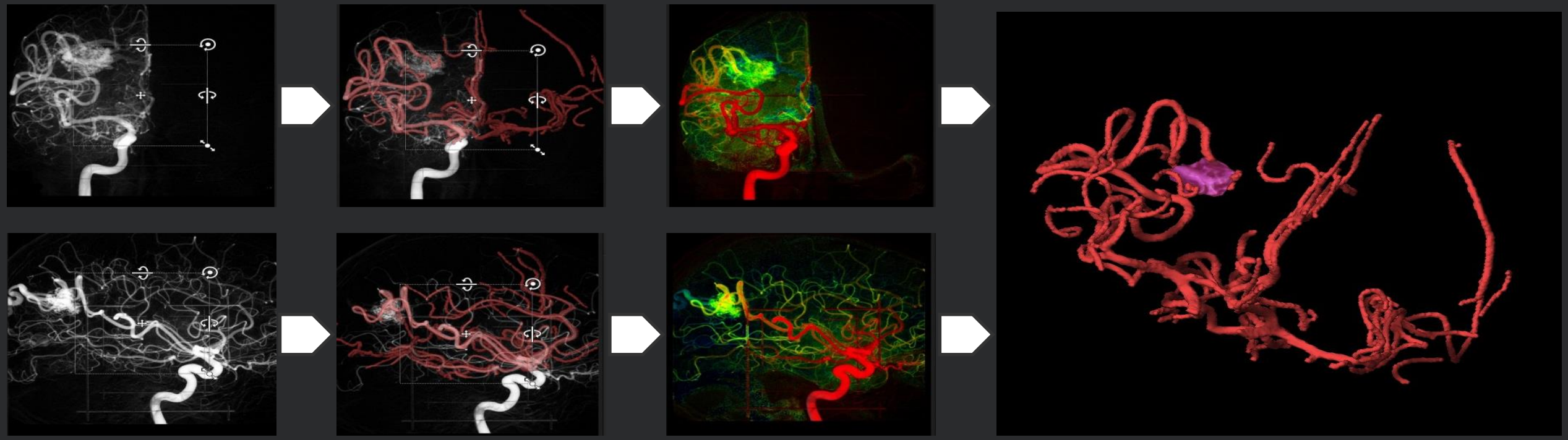

1 2D TO 3D VESSEL TREE FUSION

2 COLOR INTENSITY PROJECTION ROI

3 AUTOMATIC NIDUS SEGMENTATION

2D TO 3D VESSEL TREE FUSION

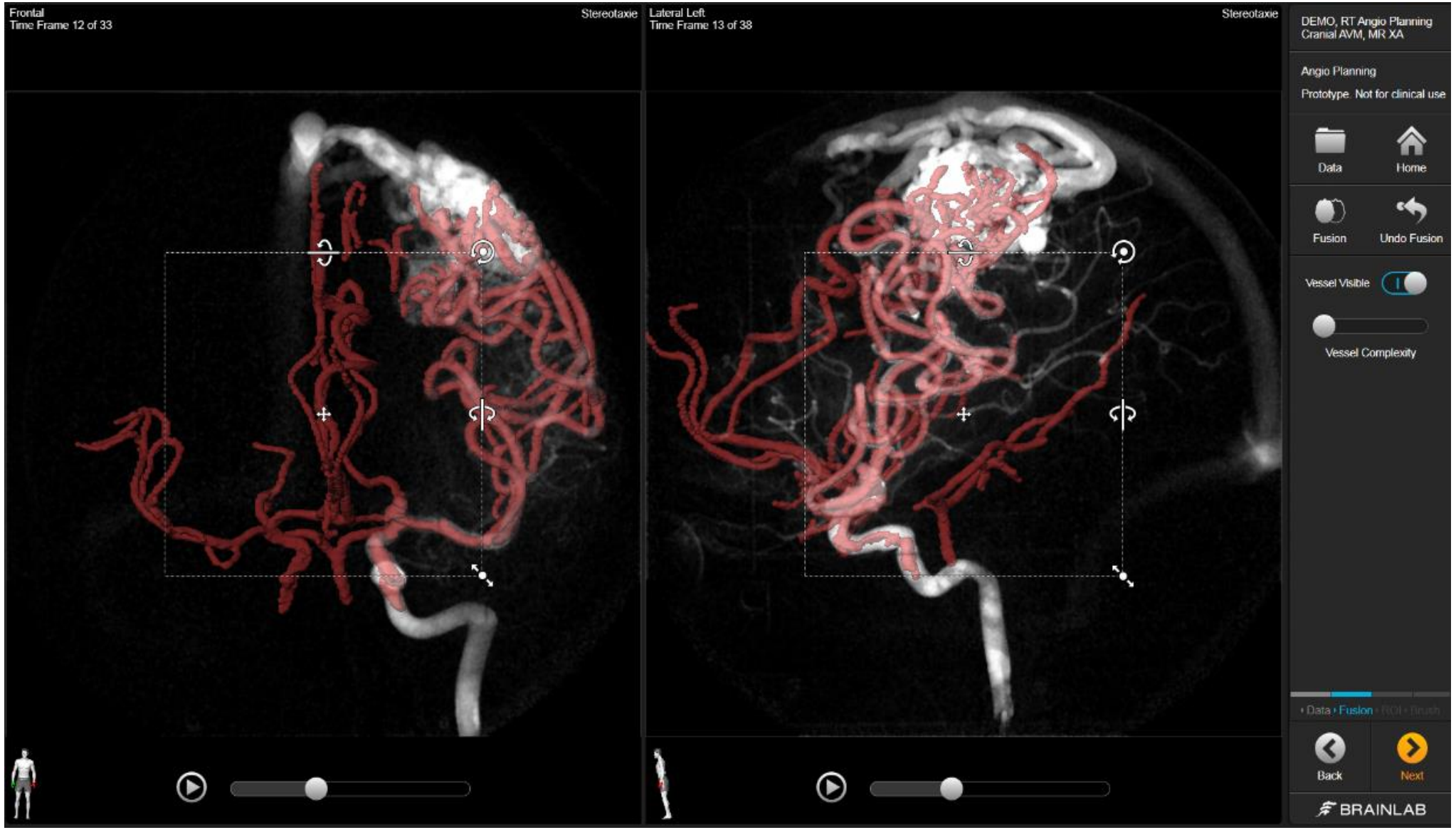

ROI OUTLINING

Color Intensity Projection (CIP) view

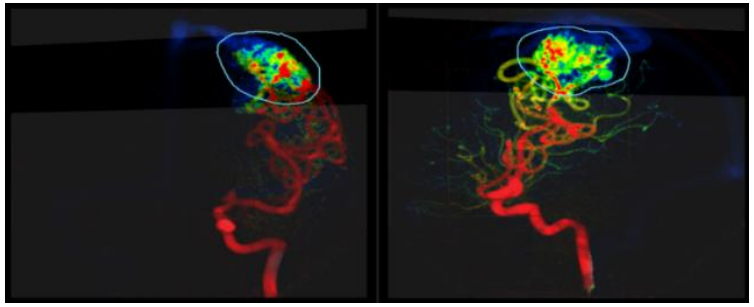

NIDUS GENERATION

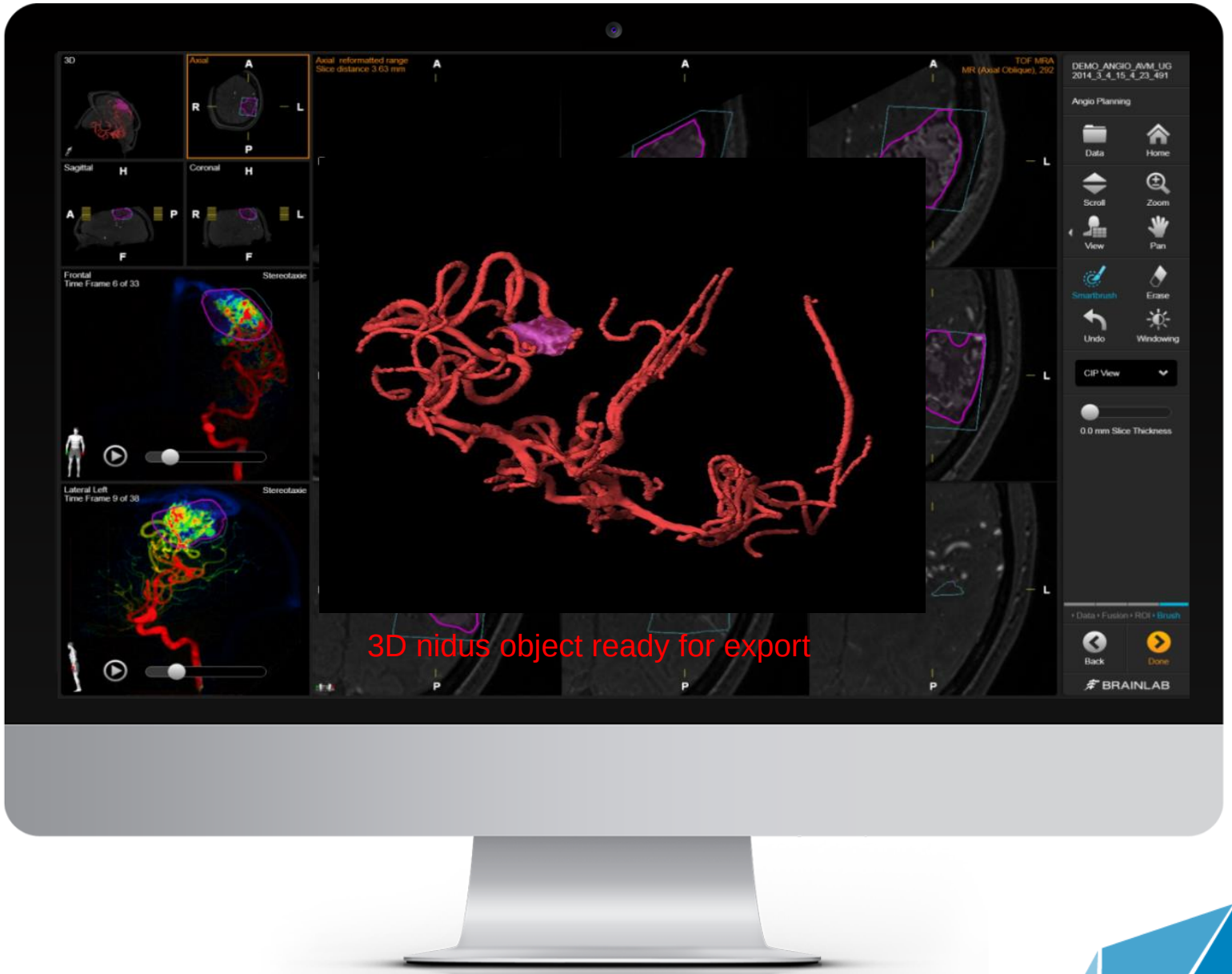

BRAINLAB

BRAINLAB ELEMENTS

FIBERTRACKING

FIBERTRACKING

FUNCTIONAL PLANNING ELEMENT

- Completamente automatizzato e DTI Data Preprocessing migliorato: Motion- / Eddy Current Correction, Denoising, Riallineamento B-Vector.
- Supporto di Fusione Elastica
- Accesso veloce & intuitivo all´atlas-based inclusione/esclusione del Tracking delle ROI
- Vista Brain Projection per una pianificazione funzionale intuitiva e revisione
- Fibertracking “On-the-Fly”

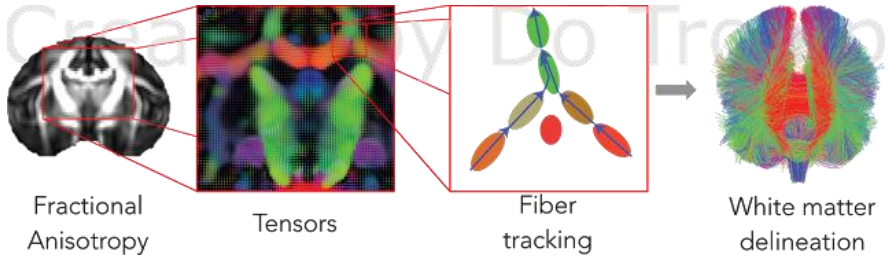

BRAINLAB

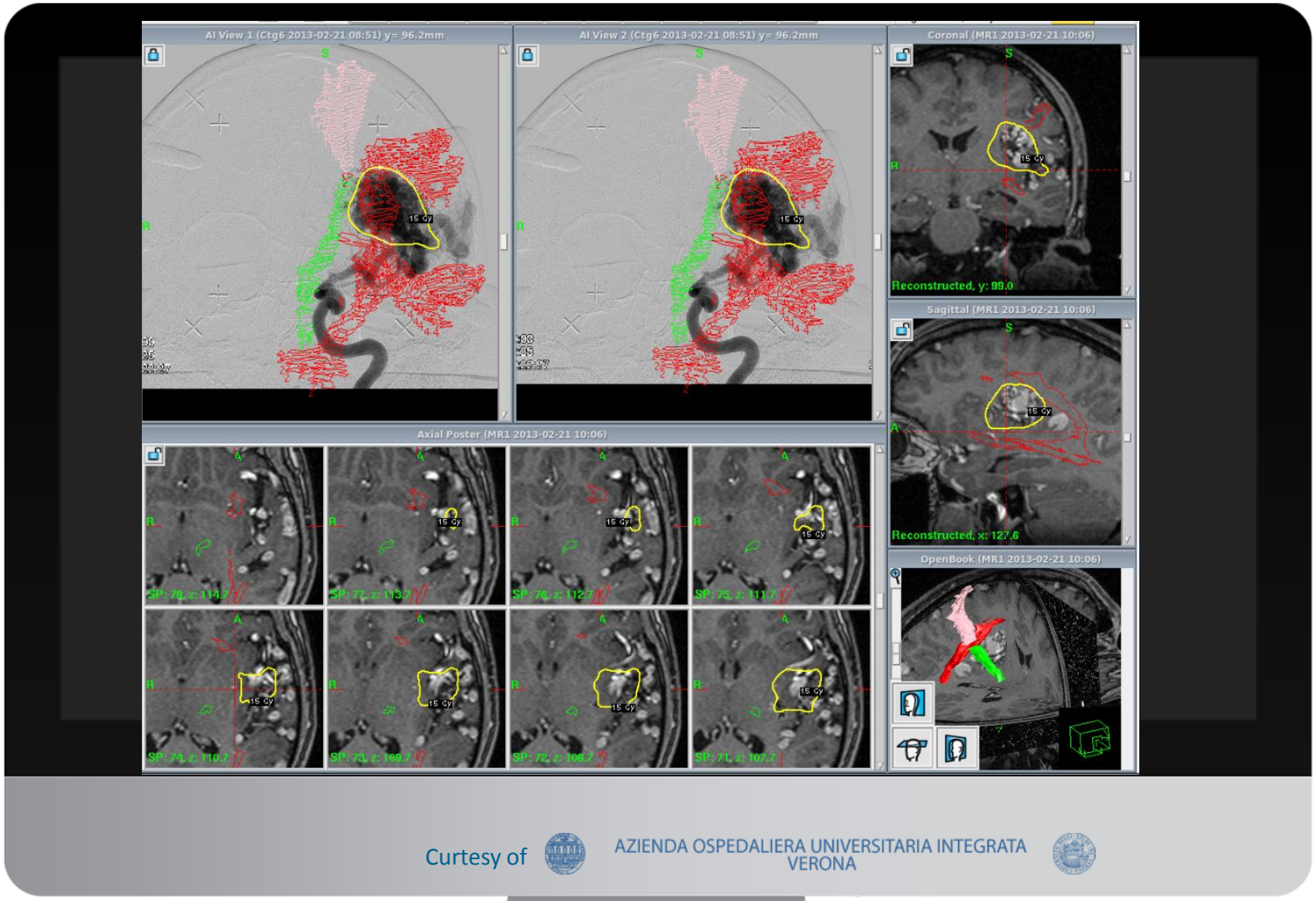
AI View 1 (Ctg6 2013-02-21 08:51) y= 96.2mm
AI View 2 (Ctg6 2013-02-21 08:51) y= 96.2mm
Coronal (MR1 2013-02-21 10:06)
Reconstructed, y: 99.0
Sagittal (MR1 2013-02-21 10:06)
Reconstructed, x: 127.6
Axial Poster (MR1 2013-02-21 10:06)
OpenBook (MR1 2013-02-21 10:06)
15 Gy
Curtesy of
AZIENDA OSPEDALIERA UNIVERSITARIA INTEGRATA
VERONA

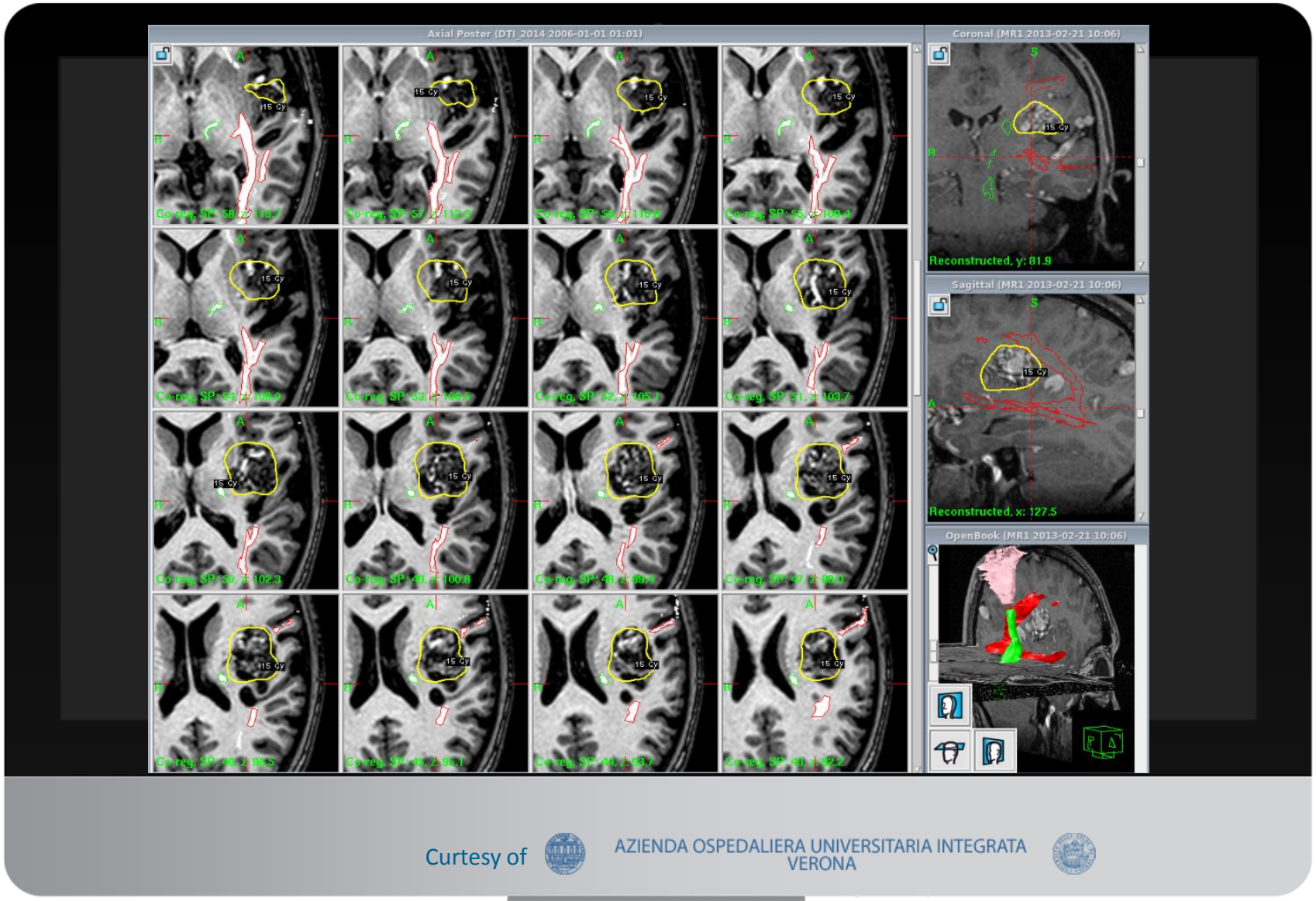
Axial Poster (DTI_2014 2006-01-01 01:01)
Coronal (MR1 2013-02-21 10:06)
Reconstructed, y: 81.9
Sagittal (MR1 2013-02-21 10:06)
Reconstructed, x: 127.5
OpenBook (MR1 2013-02-21 10:06)
Curtesy of
AZIENDA OSPEDALIERA UNIVERSITARIA INTEGRATA
VERONA

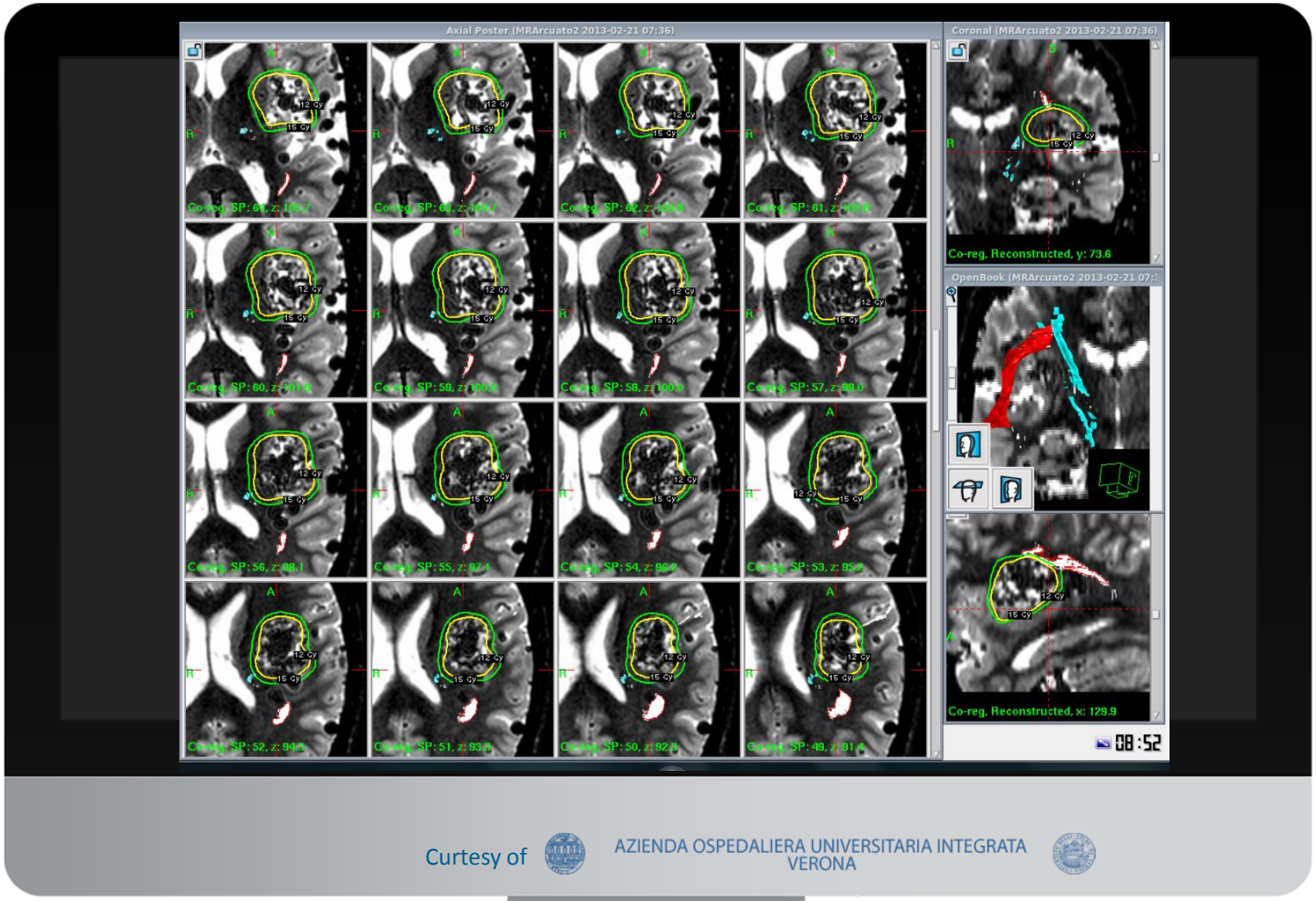
Axial Poster (MRArcuato2 2013-02-21 07:36)
Coronal (MRArcuato2 2013-02-21 07:36)
Co-reg, Reconstructed, y: 73.6
OpenBook (MRArcuato2 2013-02-21 07:
Co-reg, Reconstructed, x: 129.9
08:52
Curtesy of
AZIENDA OSPEDALIERA UNIVERSITARIA INTEGRATA
VERONA

Photon and proton therapy planning comparison for malignant glioma based on CT, FDG-PET, DTI-MRI and fiber tracking

Per Munck af Rosenschöld Radiation Medicine Research Center, Department of Radiation Oncology, Rigshospitalet, Copenhagen, DenmarkCorrespondenceper.munck@rh.regionh.dk
Silke Engelholm *Radiation Medicine Research Center, Department of Radiation Oncology, Rigshospitalet, Copenhagen, Denmark*, Lars Ohlhues *Radiation Medicine Research Center, Department of Radiation Oncology, Rigshospitalet, Copenhagen, Denmark*, Ian Law *Department of Clinical Physiology, Nuclear Medicine and PET, Rigshospitalet, Copenhagen, Denmark*, Ivan Vogelius *Radiation Medicine Research Center, Department of Radiation Oncology, Rigshospitalet, Copenhagen, Denmark* & Svend Aage Engelholm *Radiation Medicine Research Center, Department of Radiation Oncology, Rigshospitalet, Copenhagen, Denmark*

- **Pages 777-783 | Received 16 Mar 2011, Accepted 13 Apr 2011, Published online: 18 Jul 2011**

Abstract

Purpose. The purpose of this study was to compare treatment plans generated using fixed beam Intensity Modulated photon Radiation Therapy (IMRT), inversely optimized arc therapy (RapidArc(R), RA) with spot-scanned Intensity Modulated Proton Therapy (IMPT) for high-grade glioma patients. Plans were compared with respect to target coverage and sparing of organs at risk (OARs), with special attention to the possibility of hippocampus sparing.

Method. Fifteen consecutive patients diagnosed with grade III and IV glioma were selected for this study. The target and OARs were delineated based on computed tomography (CT), FDG-positron emission tomography (PET) and T1-, T2-weigted, and Diffusion Tensor Imaging (DTI) magnetic resonance imaging (MRI) and fiber-tracking. In this study, a 6 MV photon beam on a linear accelerator with a multileaf collimator (MLC) with 2.5 mm leaves and a spot-scanning proton therapy machine were used. Two RA fields, using both a coplanar (clinical standard) and a non-coplanar, setup was compared to the IMRT and IMPT techniques. Three and three to four non-coplanar fields where used in the spot-scanned IMPT and IMRT plans, respectively. The same set of planning dose-volume optimizer objective values were used for the four techniques. The highest planning priority was given to the brainstem (maximum 54 Gy) followed by the PTV (prescription 60 Gy); the hippocampi, eyes, inner ears, brain and chiasm were given lower priority. Doses were recorded for the plans to targets and OARs and compared to our clinical standard technique using the Wilcoxon signed rank test.

Result. The PTV coverage was significantly more conform for IMPT than the coplanar RA technique, while RA plans tended to be more conform than the IMRT plans, as measured by the standard deviation of the PTV dose. In the cases where the tumor was confined in one cerebral hemisphere (eight patients), the non-coplanar RA and IMPT techniques yielded borderline significantly lower doses to the contralateral hippocampus compared to the standard (22% and 97% average reduction for non-coplanar RA and IMPT, respectively). The IMPT technique allowed for the largest healthy tissue sparing of the techniques in terms of whole brain doses and to the fiber tracts. The maximum doses to the chiasm and brainstem were comparable for all techniques.

Conclusion. The IMPT technique produced the most conform plans. For tumors located in the one of the cerebral hemispheres, the non-coplanar RA and the IMPT techniques were able to reduce doses to the contralateral hippocampus. The IMPT technique offered the largest sparing of the brain and fiber tracts. RA techniques tended to produce more conform target doses than IMRT.

FIBERTRACKING

"Diffusion Tensor Imaging is a cutting edge imaging technique that provides quantitative information with which to visualize and study connectivity and continuity of neural pathways in the central and peripheral nervous systems *in vivo."* (Basser et al. 2000).

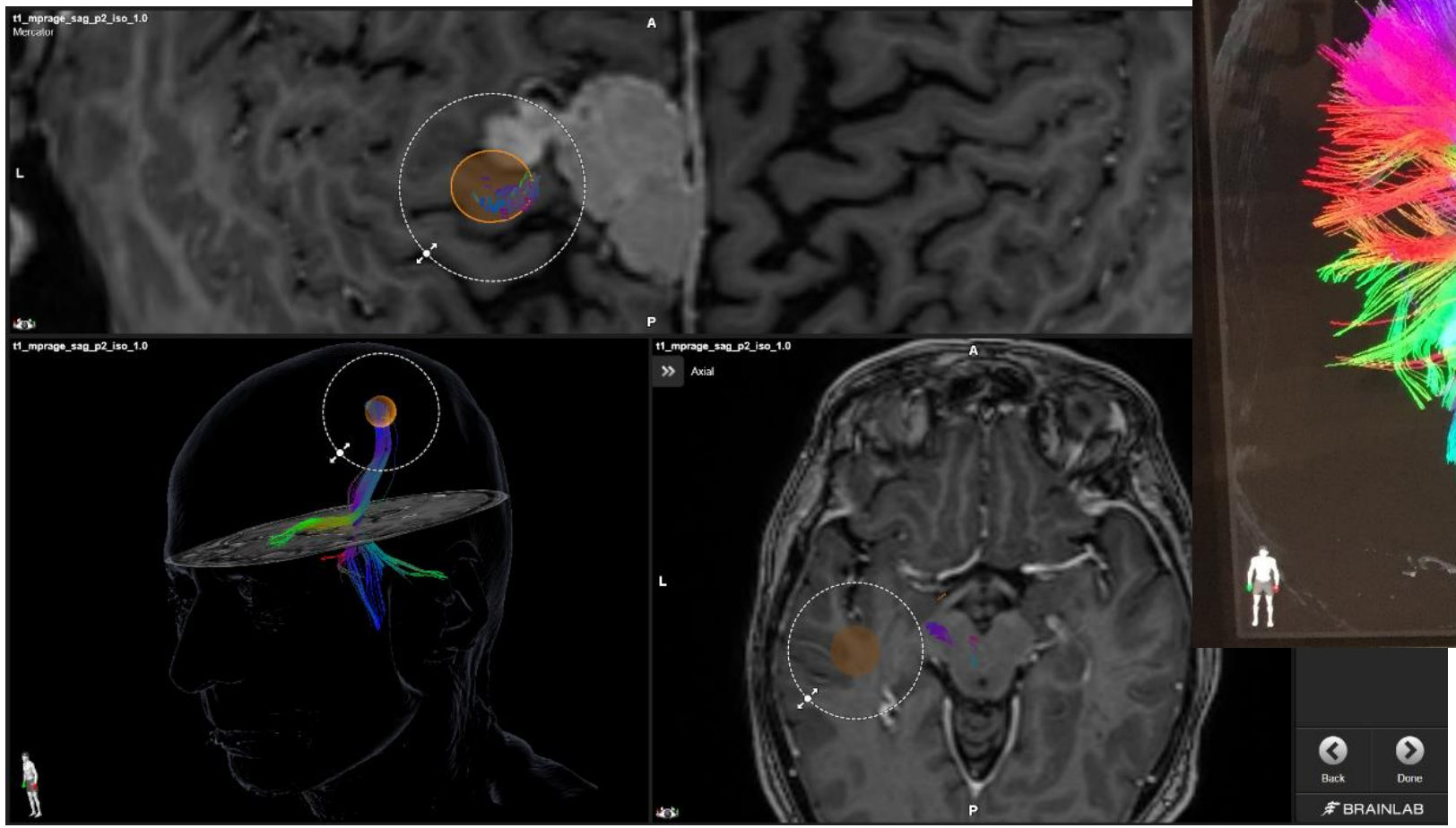

BRAINLAB ELEMENTS

4π ALGORITHM

TRAJECTORY-BASED TREATMENT PLANNING AND DELIVERY FOR CRANIAL RADIOSURGERY

JAMES ROBAR, PHD, FCCPM
LEE MACDONALD, MSC
CHRISTOPHER THOMAS, PHD, MCCPM
DALHOUSIE UNIVERSITY, CANADA

CLASS SOLUTIONS IN SRS/SRT

DALHOUSIE UNIVERSITY
Inspiring Minds
Medical Physics

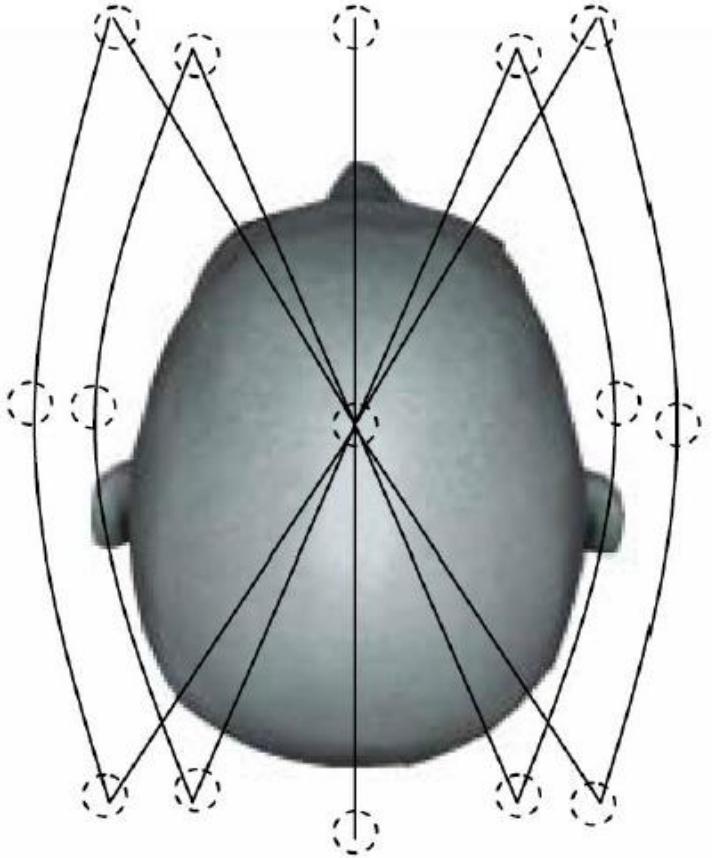

- Identical arc arrangement at cardinal angles for all cases
- No patient-specific customization to the arc arrangement
- Cranial cases are highly variable with regard to PTV and OAR geometry

PATIENT-SPECIFIC ARC TRAJECTORY

DALHOUSIE UNIVERSITY
Inspiring Minds
Medical Physics

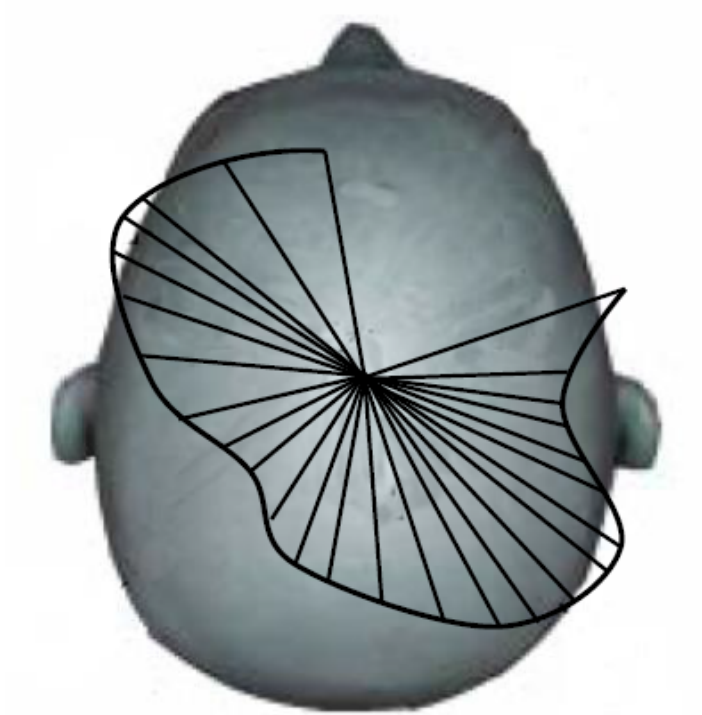

- Establish patient-tailored dynamic arc trajectories
- May involve coordinated gantry and couch motion
- Designed to minimize dose to OARs without compromising PTV coverage

FOUR CONSIDERATIONS

DALHOUSIE UNIVERSITY
Inspiring Minds
Medical Physics

Algorithm Objectives

Overlap between PTV and OAR

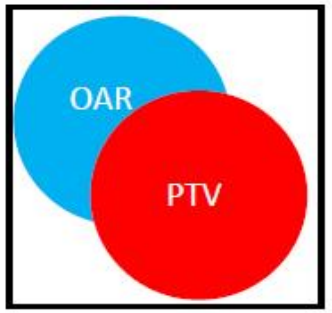

Relative Depth

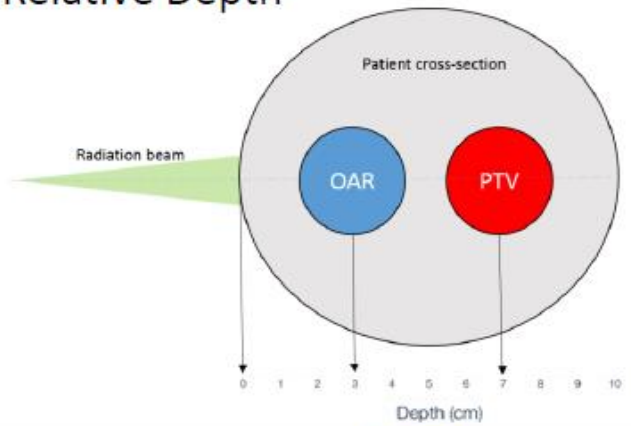

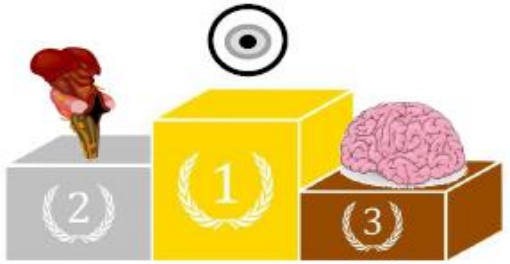

QUANTEC Dose Weighting

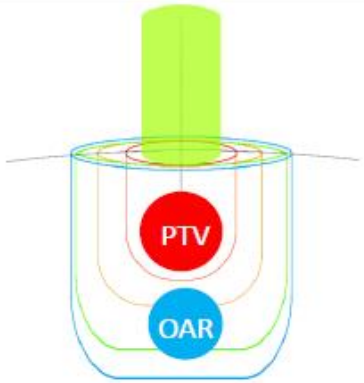

Promote Rapid Dose Fall-off

OAR OVERLAP in FOUR-PI

DALHOUSIE UNIVERSITY
Inspiring Minds
Medical Physics

- Creates a suitability ranking for every couch-gantry position
- Unique map for every patient
- Condenses three dimensional relationships between structures
- Higher penalty assigned with OAR in front of PTV

EXAMPLE: brainstem map

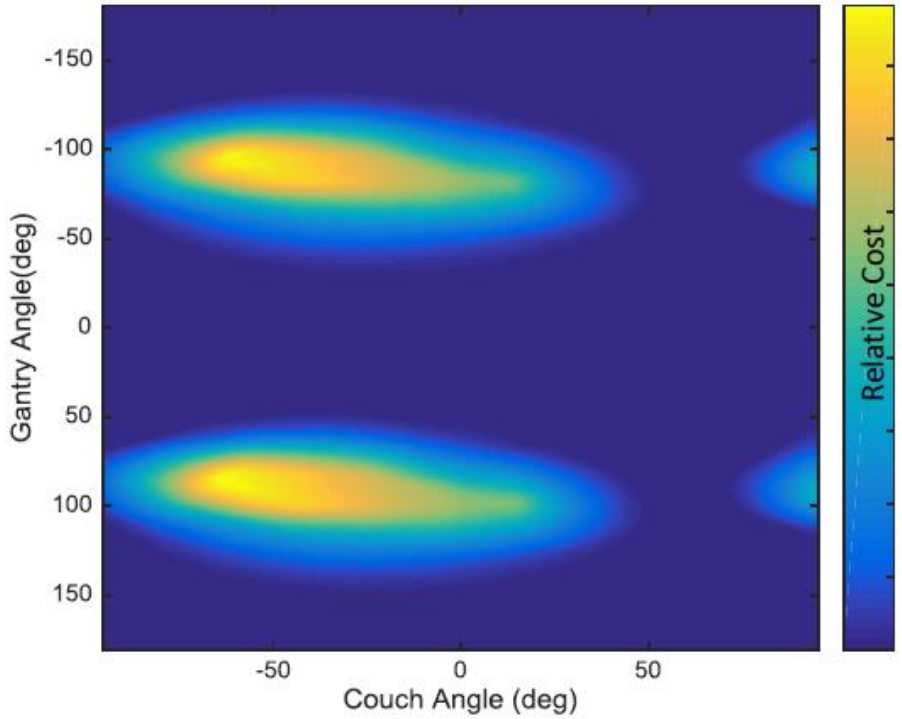

OAR OVERLAP in FOUR-PI

DALHOUSIE UNIVERSITY
Inspiring Minds
Medical Physics

A composite OAR map

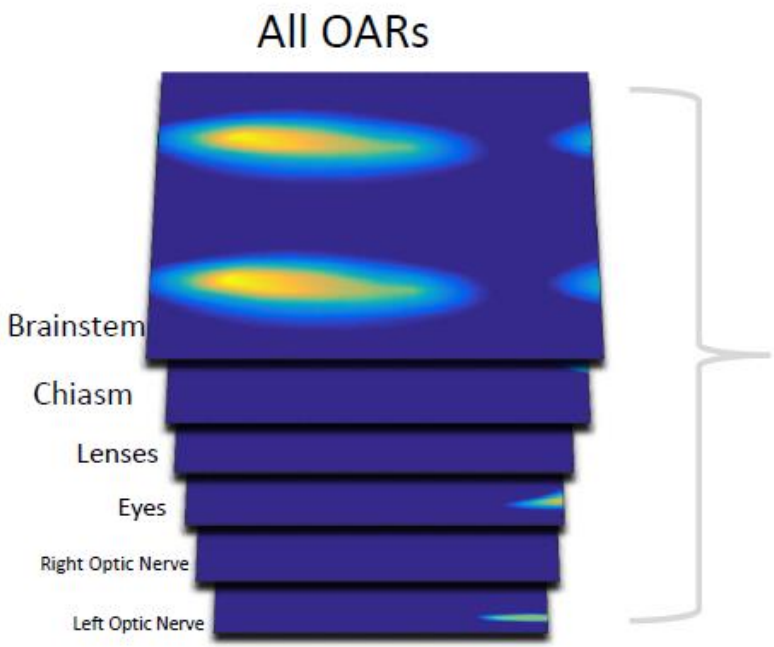

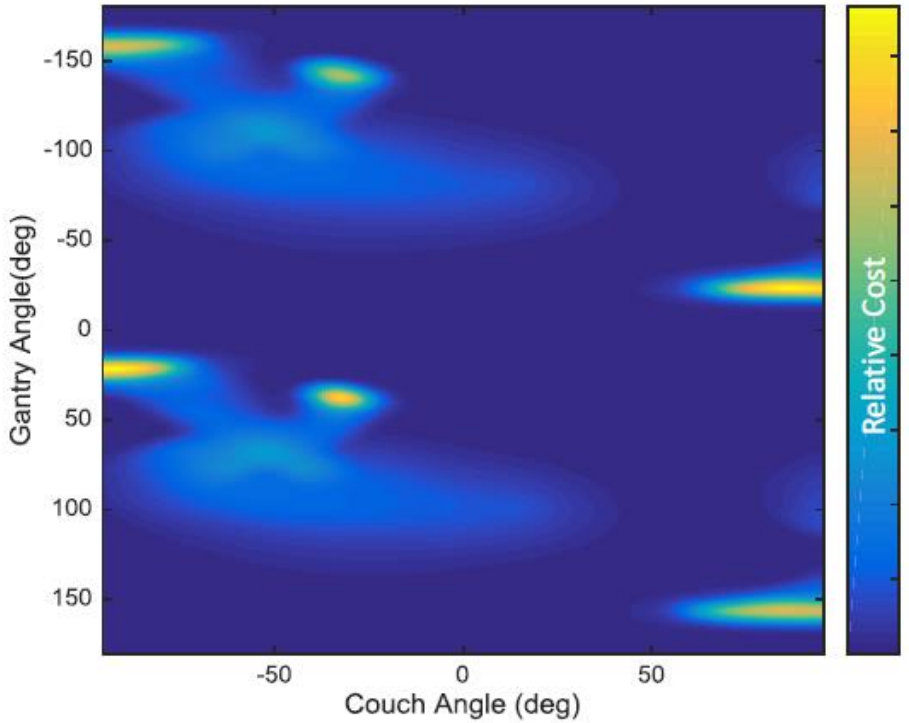

SAMPLE OVERLAP MAPS

DALHOUSIE UNIVERSITY
Inspiring Minds
Medical Physics

20 CRANIAL RADIOSURGERY PATIENTS

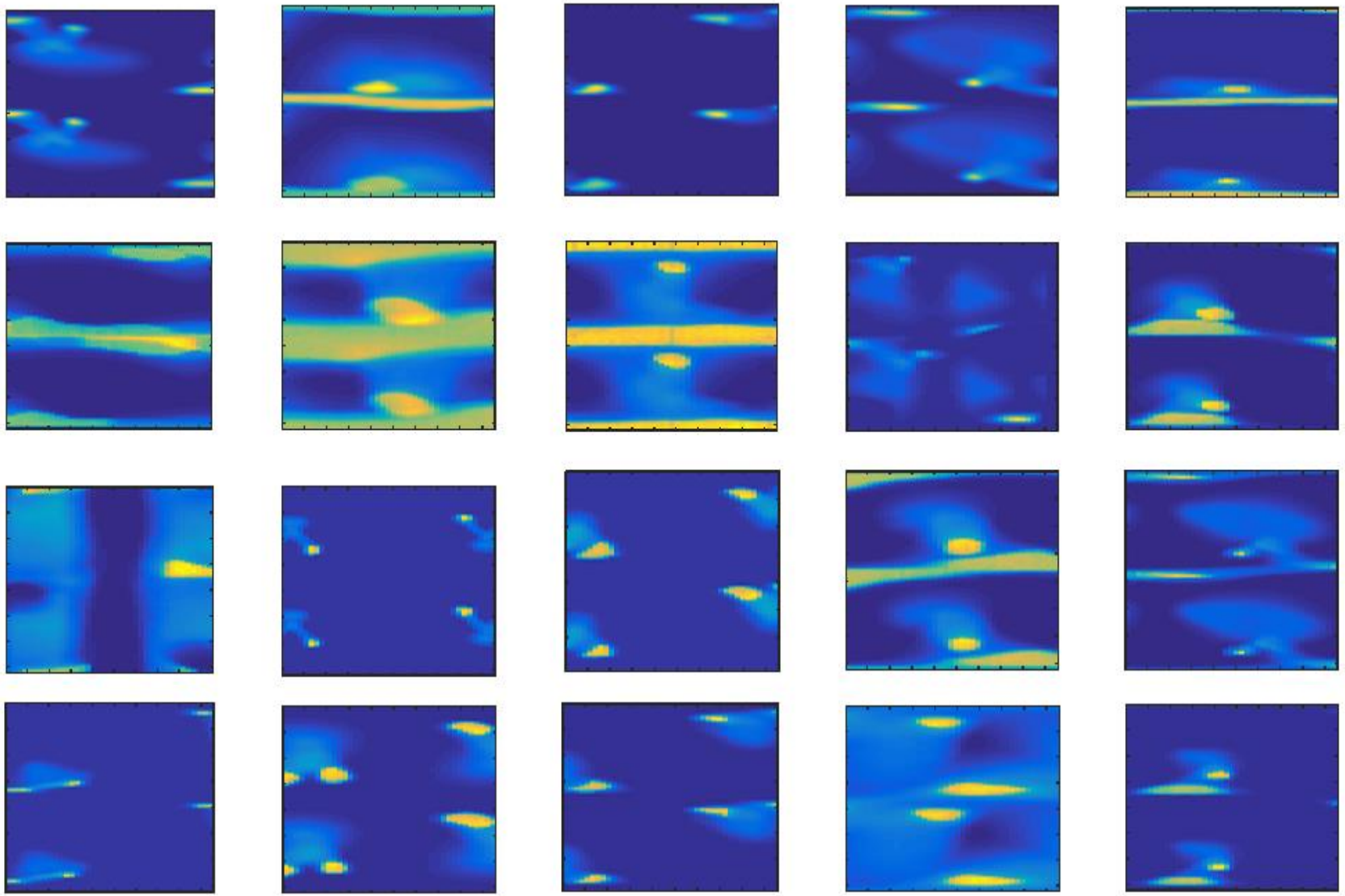

Patient Example

- Right Acoustic Neuroma.
  - Brainstem
  - Eyes
  - Lenses
  - Optic Chiasm
  - Optic Nerves

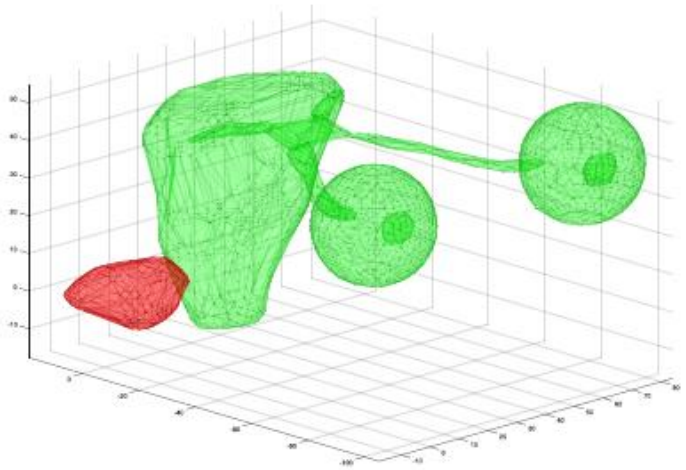

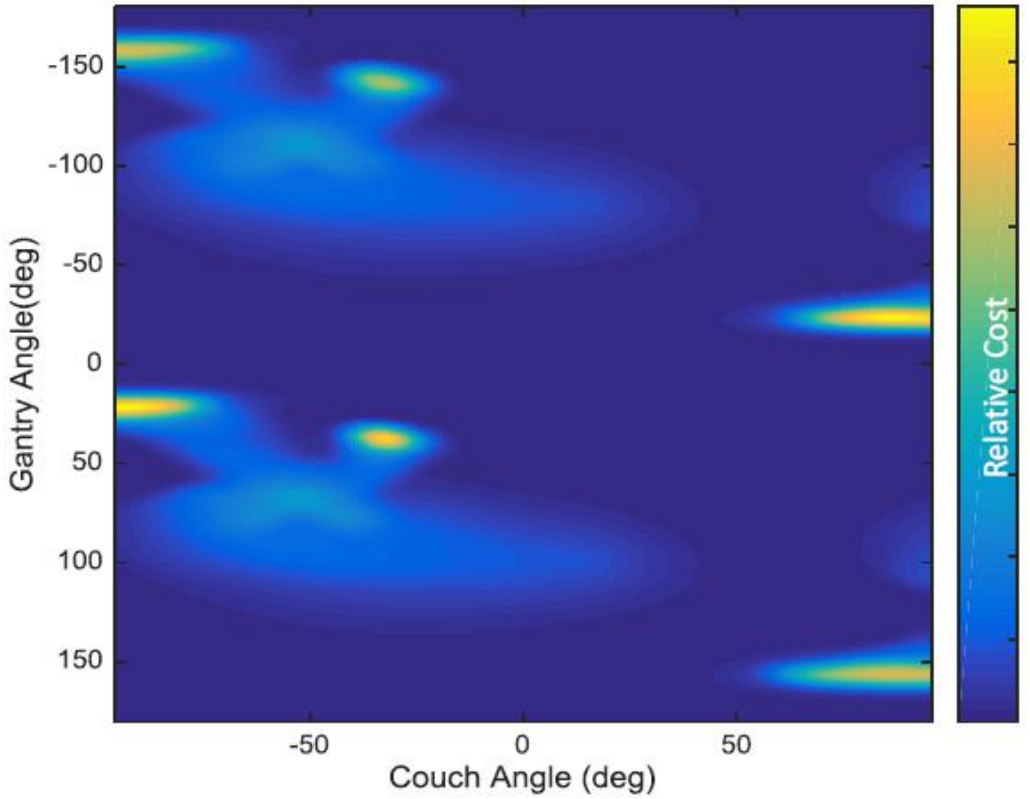

NAVIGATION OF THE MAP

DALHOUSIE UNIVERSITY
Inspiring Minds
Medical Physics

Conventional Class Solution

Standard cranial template

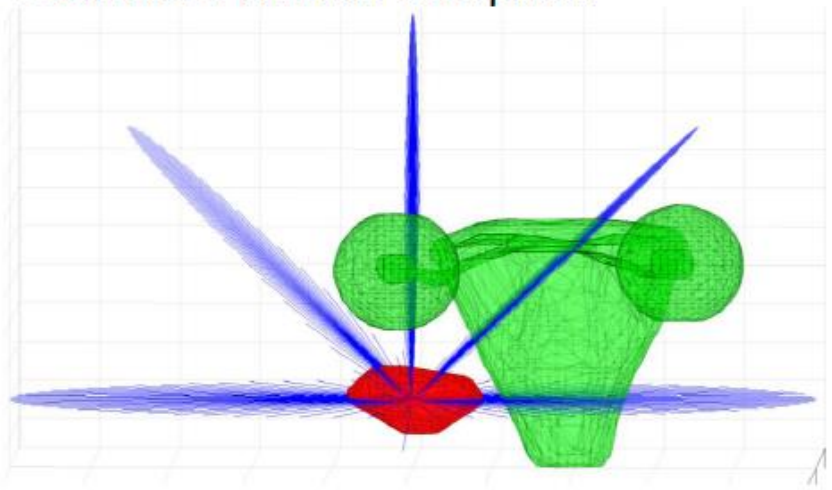

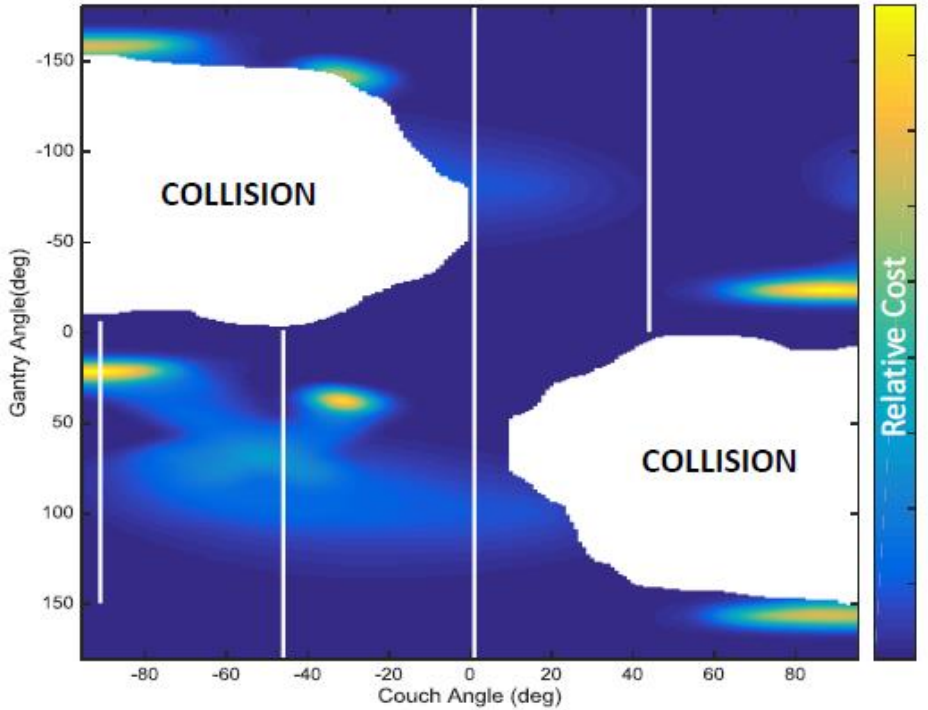

NAVIGATION OF THE MAP

DALHOUSIE UNIVERSITY
Inspiring Minds
Medical Physics

Fixed-Couch Optimization

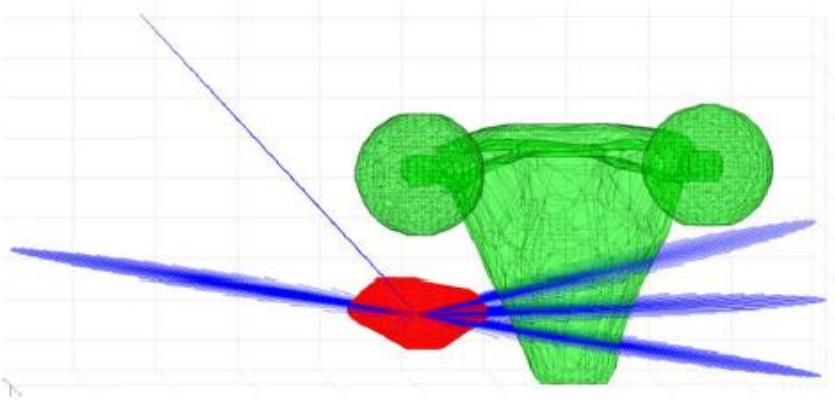

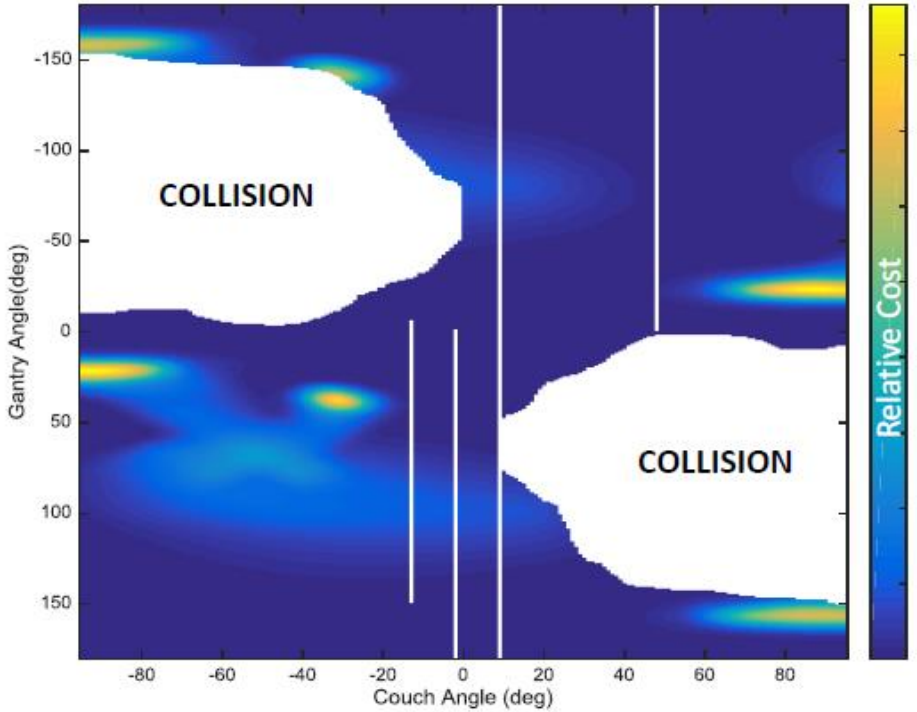

DYNAMIC TRAJECTORY

DALHOUSIE UNIVERSITY
Inspiring Minds
Medical Physics

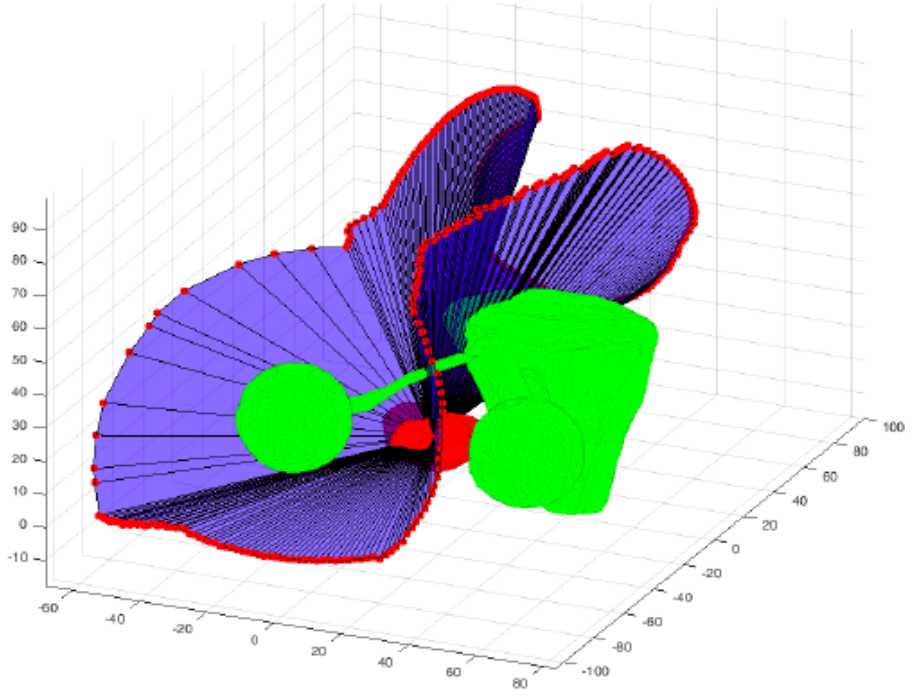

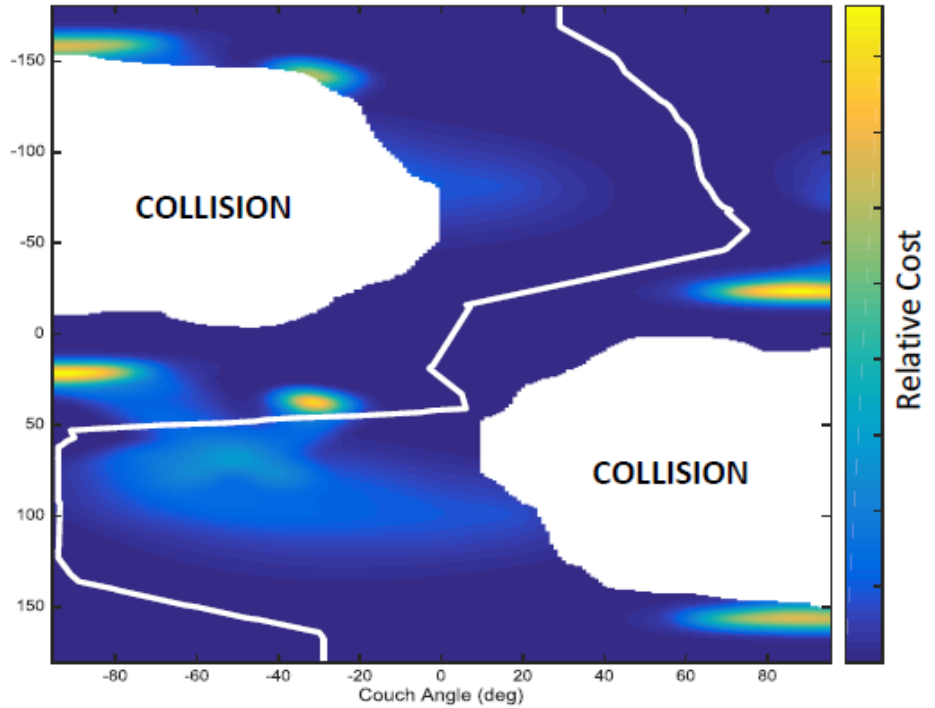

FourPi in BRAINLAB CRANIAL SRS ELEMENT

DALHOUSIE UNIVERSITY
Inspiring Minds
Medical Physics

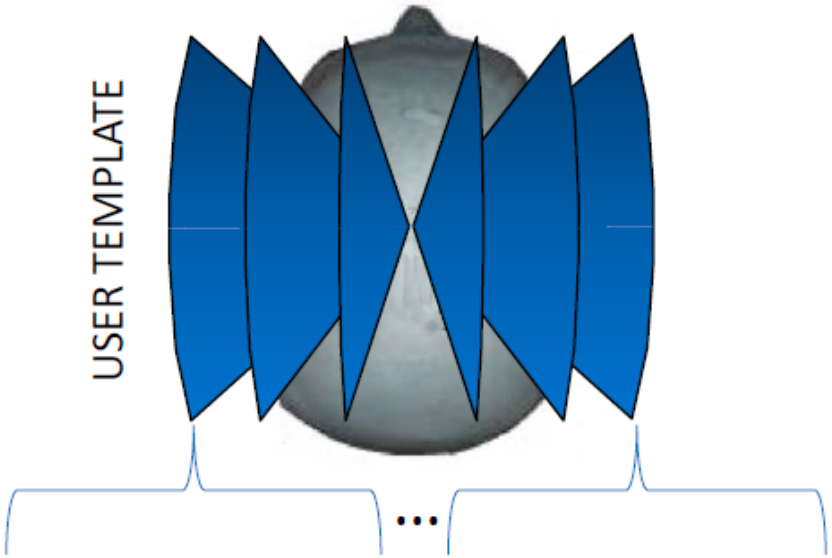

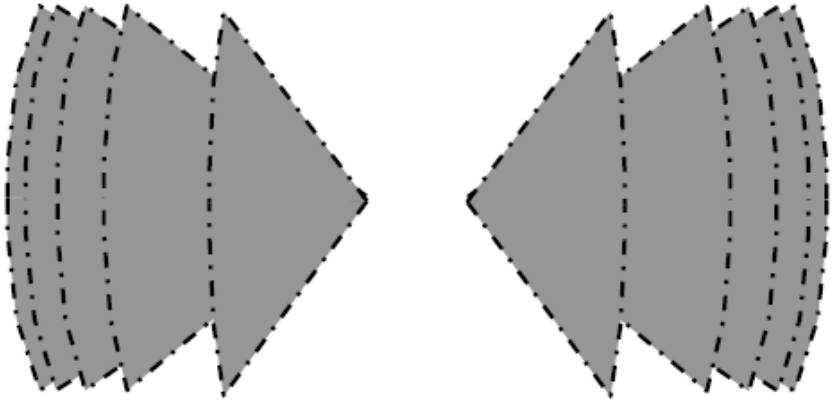

FIND ALL POSSIBLE ARCS

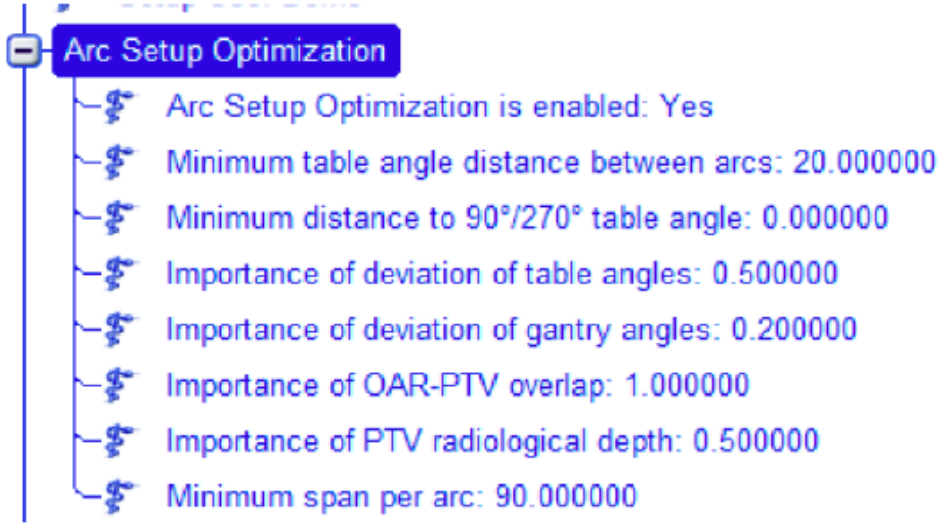

FIND BEST POSSIBLE SET

- PTV/OAR overlap
- OAR radiological depth
- OAR on source side
- Gantry stop/start deviations
- Table deviations

ASSIGN PENALTIES

BRAINLAB

EXACTRAC X-RAY

PRECISIONE

EXACTRAC X-RAY

EXACTRAC X-RAY

NON-COPLANAR IMAGE-GUIDED MONITORING

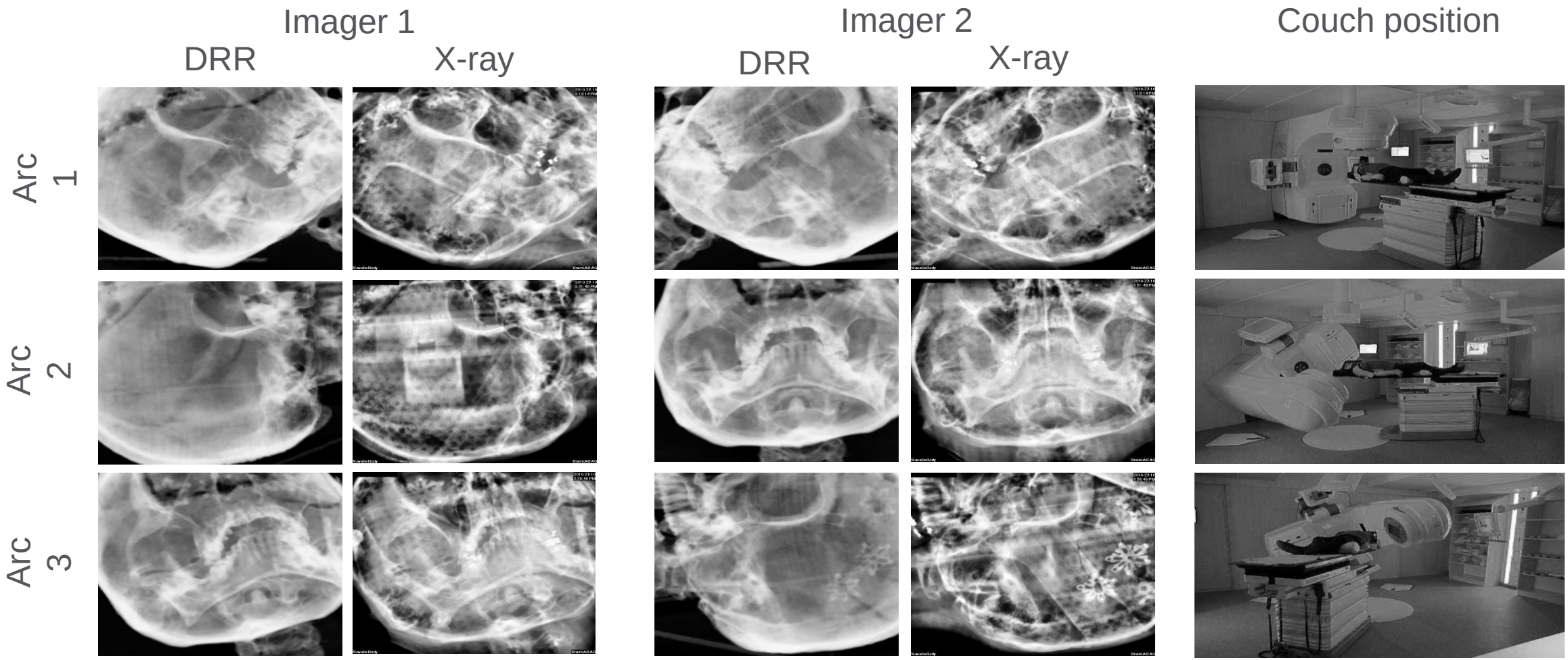

EXACTRAC X-RAY

GK → sorgenti multiple CO60

CK → linac based con reticolo di punti

Distribuzione della dose per limitare la tossicita´agli OAR ed ottimizzare CI

LINAC → tecnica ad archi non co-planari

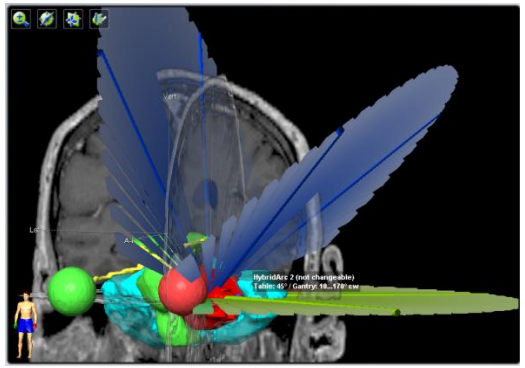

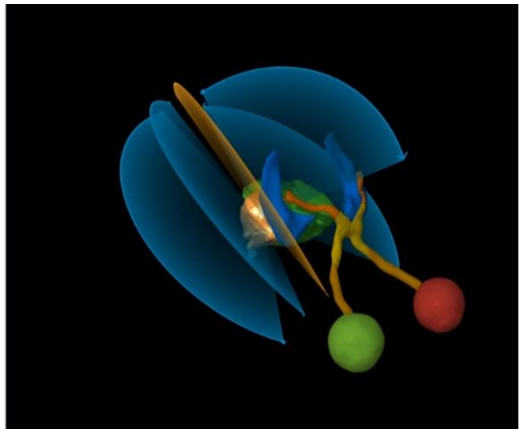

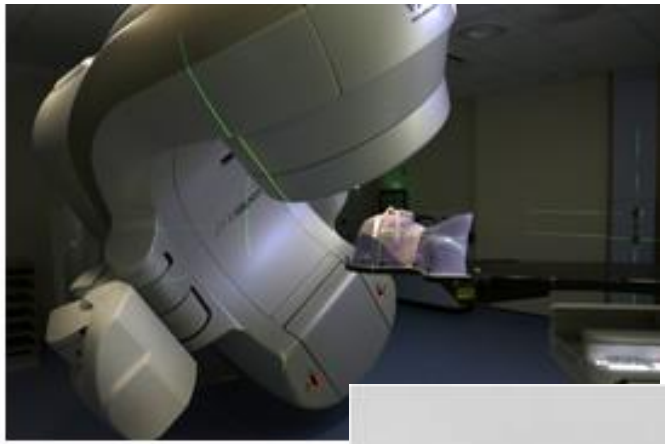

J Neurosurg. 2004 Nov;101 Suppl 3:351-5

Geometrical accuracy of the Novalis stereotactic radiosurgery system for trigeminal neuralgia.

•Rahimian J[1], Chen JC, Rao AA, Girvigian MR, Miller MJ, Greathouse HE.

Author information

•[1]Departments of Radiation Oncology and Neurological Surgery, Southern California Permanente Medical Group, Los Angeles, 90027, USA. Javad.X.Rahimian@KP.org

Abstract

OBJECT:

Stringent geometrical accuracy and precision are required in the stereotactic radiosurgical treatment of patients. Accurate targeting is especially important when treating a patient in a single fraction of a very high radiation dose (90 Gy) to a small target such as that used in the treatment of trigeminal neuralgia (3 to 4-mm diameter). The purpose of this study was to determine the inaccuracies in each step of the procedure including imaging, fusion, treatment planning, and finally the treatment. The authors implemented a detailed quality-assurance program.

METHODS:

Overall geometrical accuracy of the Novalis stereotactic system was evaluated using a Radionics Geometric Phantom Chamber. The phantom has several magnetic resonance (MR) and computerized tomography (CT) imaging-friendly objects of various shapes and sizes. Axial 1-mm-thick MR and CT images of the phantom were acquired using a T1-weighted three-dimensional spoiled gradient recalled pulse sequence and the CT scanning protocols used clinically in patients. The absolute errors due to MR image distortion, CT scan resolution, and the image fusion inaccuracies were measured knowing the exact physical dimensions of the objects in the phantom. The isocentric accuracy of the Novalis gantry and the patient support system was measured using the Winston-Lutz test. Because inaccuracies are cumulative, to calculate the system's overall spatial accuracy, the root mean square (RMS) of all the errors was calculated. To validate the accuracy of the technique, a 1.5-mm-diameter spherical marker taped on top of a radiochromic film was fixed parallel to the x-z plane of the stereotactic coordinate system inside the phantom. The marker was defined as a target on the CT images, and seven noncoplanar circular arcs were used to treat the target on the film. The calculated system RMS value was then correlated with the position of the target and the highest density on the radiochromic film. The mean spatial errors due to image fusion and MR imaging were 0.41+/-0.3 and 0.22+/-0.1 mm, respectively. Gantry and couch isocentricities were 0.3+/-0.1 and 0.6+/-0.15 mm, respectively. The system overall RMS values were 0.9 and 0.6 mm with and without the couch errors included, respectively (isocenter variations due to couch rotation are microadjusted between couch positions). The positional verification of the marker was within 0.7+/-0.1 mm of the highest optical density on the radiochromic film, correlating well with the system's overall RMS value. The overall mean system deviation was 0.32+/-0.42 mm.

CONCLUSIONS:

The highest spatial errors were caused by image fusion and gantry rotation. A comprehensive quality-assurance program was developed for the authors' stereotactic radiosurgery program that includes medical imaging, linear accelerator mechanical isocentricity, and treatment delivery. For a successful treatment of trigeminal neuralgia with a 4-mm cone, the overall RMS value of equal to or less than 1 mm must be guaranteed.

EXACTRAC PROPOSITION
SUPERIOR MONITORING ACCURACY

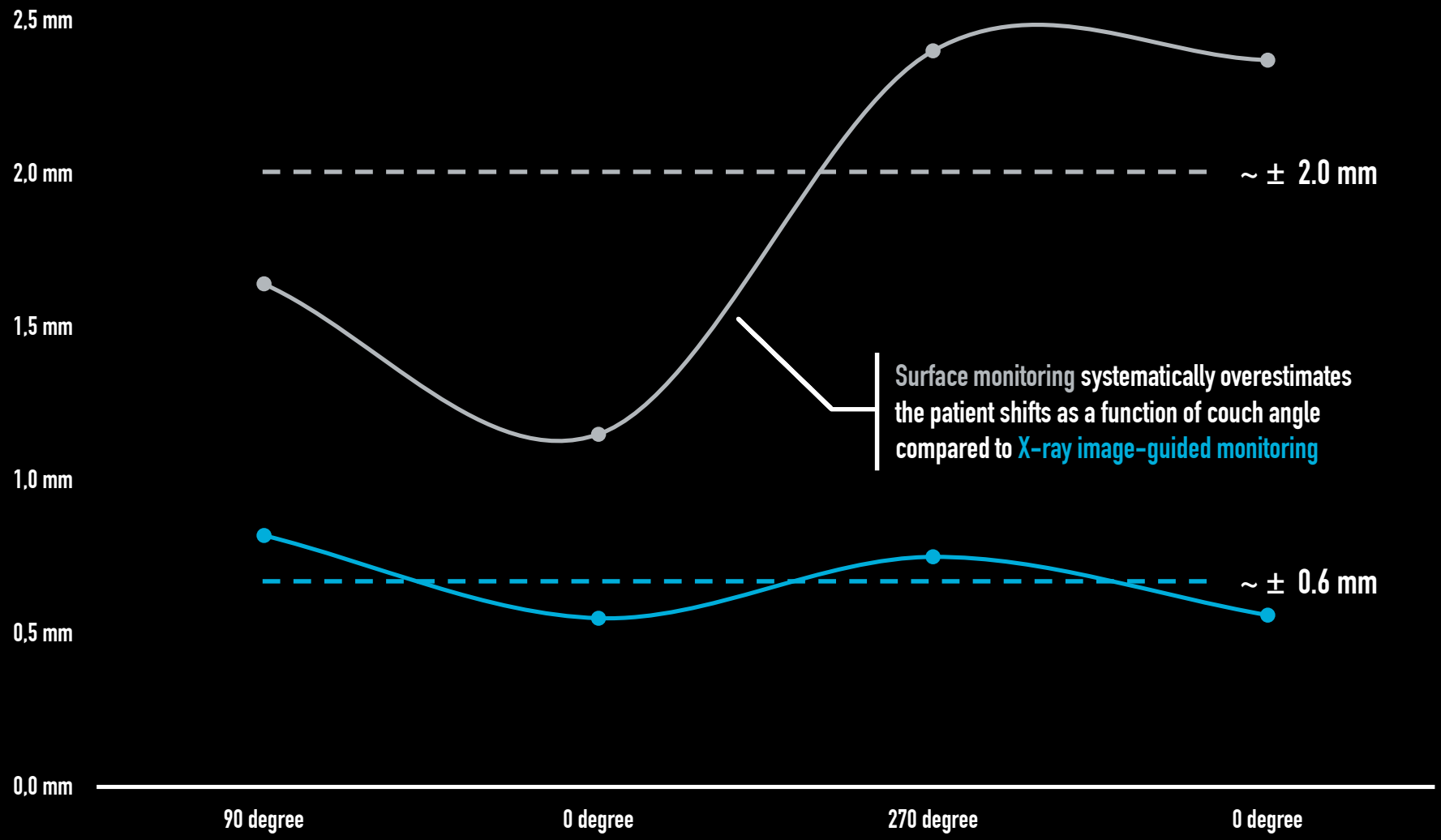

Gevaert, T. et al. Evaluation of the clinical usefulness for using verification images during frameless radiosurgery. Radiother. Oncol. 108, 114–7 (2013).

DOSIMETRIC IMPACT OF REMAINING ROTATIONS
EXAMPLE OF A THIRTHEEN BRAIN METASTASES CASE

DVH ANALYSIS
TRANSLATIONAL DEVIATIONS

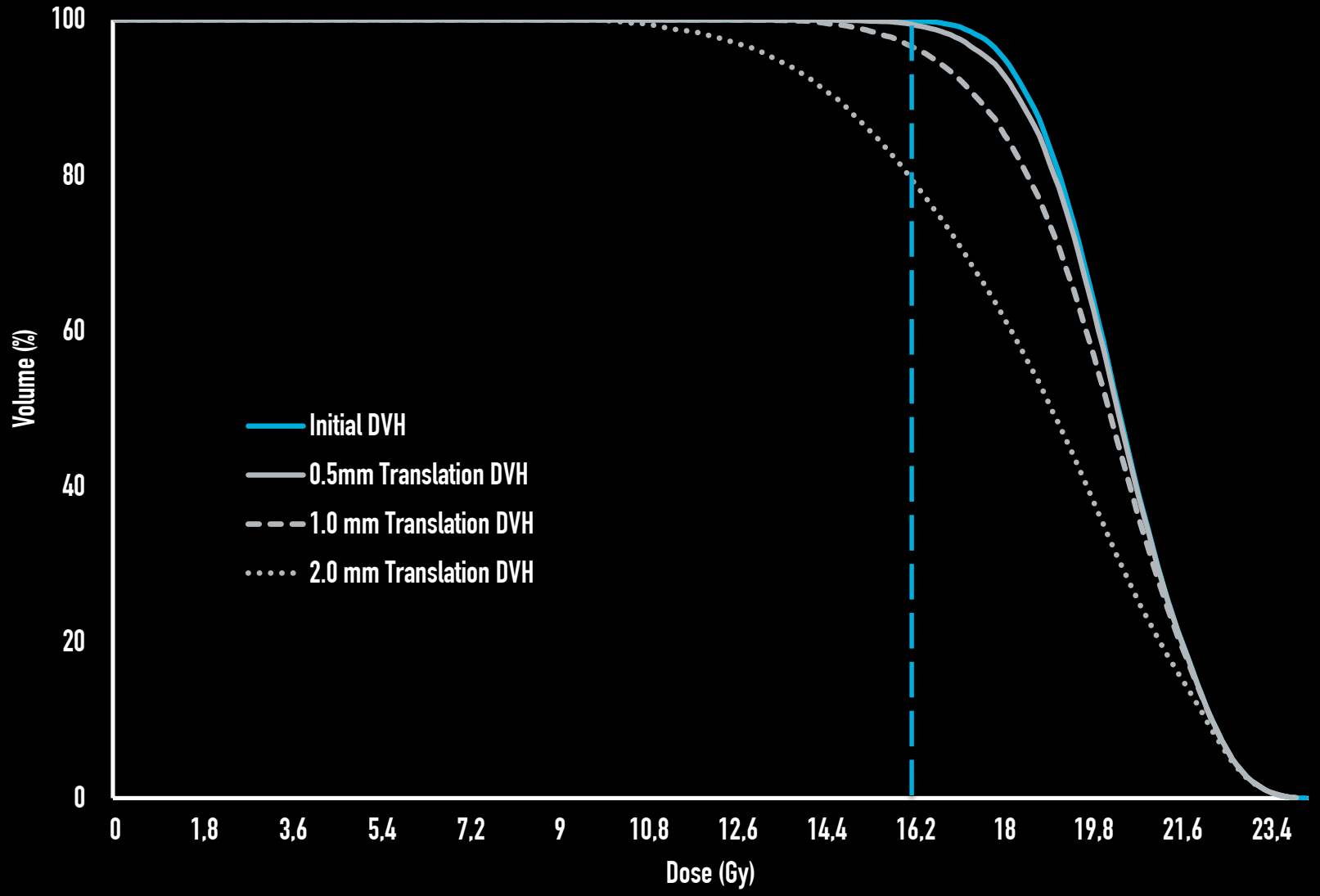

DVH ANALYSIS
ROTATIONAL DEVIATIONS

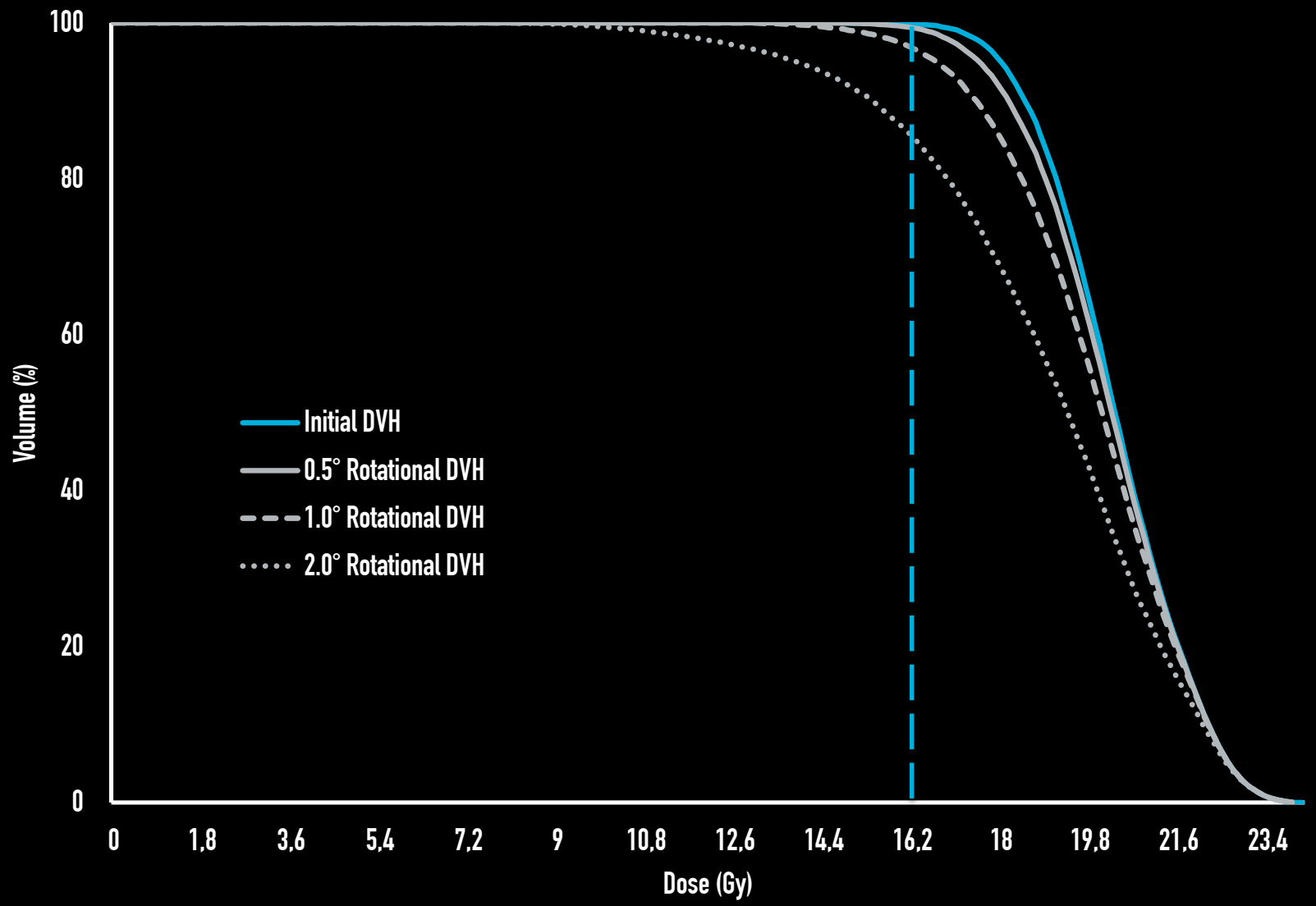

Accuracy of surface registration compared to conventional volumetric registration in patient positioning for head-and-neck radiotherapy: A simulation study using patient data

Youngjun Kim[1], Ruijiang Li[2], Yong Hum Na[2], Rena Lee[3,a)] and Lei Xing[4]

- Purpose: 3D optical surface imaging has been applied to patient positioning in radiation therapy (RT). The optical patient positioning system is advantageous over conventional method using cone-beam computed tomography (CBCT) in that it is radiation free, frameless, and is capable of real-time monitoring. While the conventional radiographic method uses volumetric registration, the optical system uses surface matching for patient alignment. The relative accuracy of these two methods has not yet been sufficiently investigated. This study aims to investigate the theoretical accuracy of the surface registration based on a simulation study using patient data.
- Methods: This study compares the relative accuracy of surface and volumetric registration in head-and-neck RT. The authors examined 26 patient data sets, each consisting of planning CT data acquired before treatment and patient setup CBCT data acquired at the time of treatment. As input data of surface registration, patient's skin surfaces were created by contouring patient skin from planning CT and treatment CBCT. Surface registration was performed using the iterative closest points algorithm by point–plane closest, which minimizes the normal distance between source points and target surfaces. Six degrees of freedom (three translations and three rotations) were used in both surface and volumetric registrations and the results were compared. The accuracy of each method was estimated by digital phantom tests.
- Results: Based on the results of 26 patients, the authors found that the average and maximum root-mean-square translation deviation between the surface and volumetric registrations were 2.7 and 5.2 mm, respectively. The residual error of the surface registration was calculated to have an average of 0.9 mm and a maximum of 1.7 mm.
- Conclusions: Surface registration may lead to results different from those of the conventional volumetric registration. Only limited accuracy can be achieved for patient positioning with an approach based solely on surface information.

VisionRT / C-RAD technology scrutinized by Stanford

The inferiority of surface scanning has been demonstrated for the first time on real patient data. The Stanford team published a comparison between surface matching and volume matching (CBCT) for 26 H&N patients and warn for the significant errors associated with surface scanning.

Accuracy of surface registration compared to conventional volumetric registration in patient positioning for head-and-neck radiotherapy: A simulation study using patient data.

26 H&N Patients
Retrospective analysis
Varian TrueBeam Linac
Stanford School of Medicine

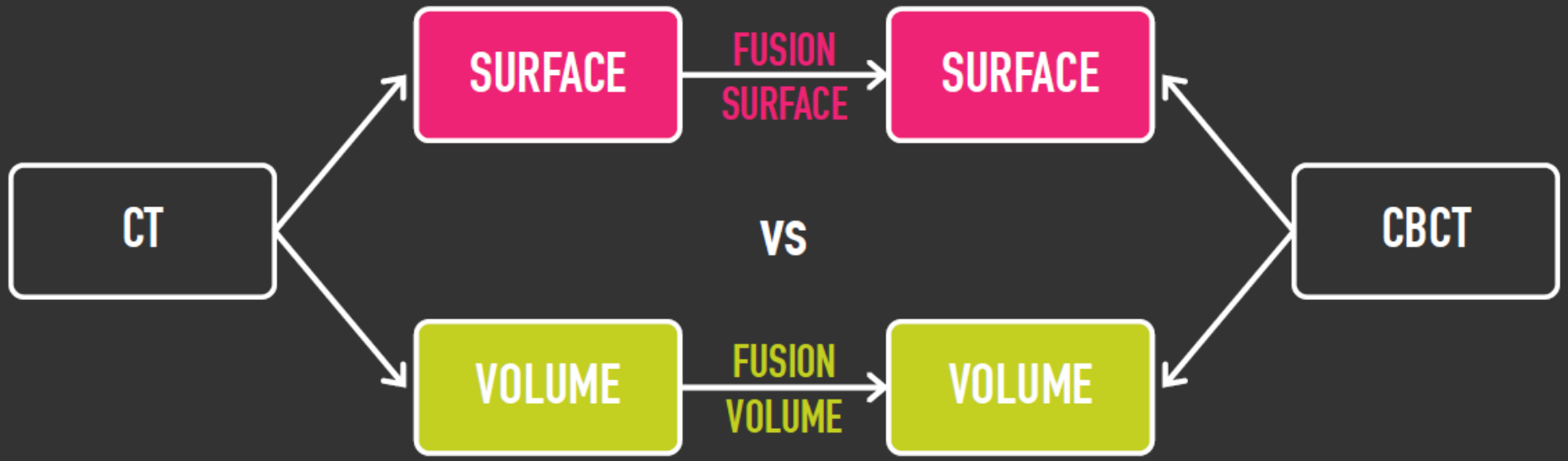

Kim, Y., Li, R., Na, Y. H., Lee, R. & Xing, L. Accuracy of surface registration compared to conventional volumetric registration in patient positioning for head-and-neck radiotherapy: A simulation study using patient data. Med. Phys. 41, 121701 (2014).

EXACTRAC PROPOSITION
SUPERIOR MONITORING ACCURACY

BRAINLAB

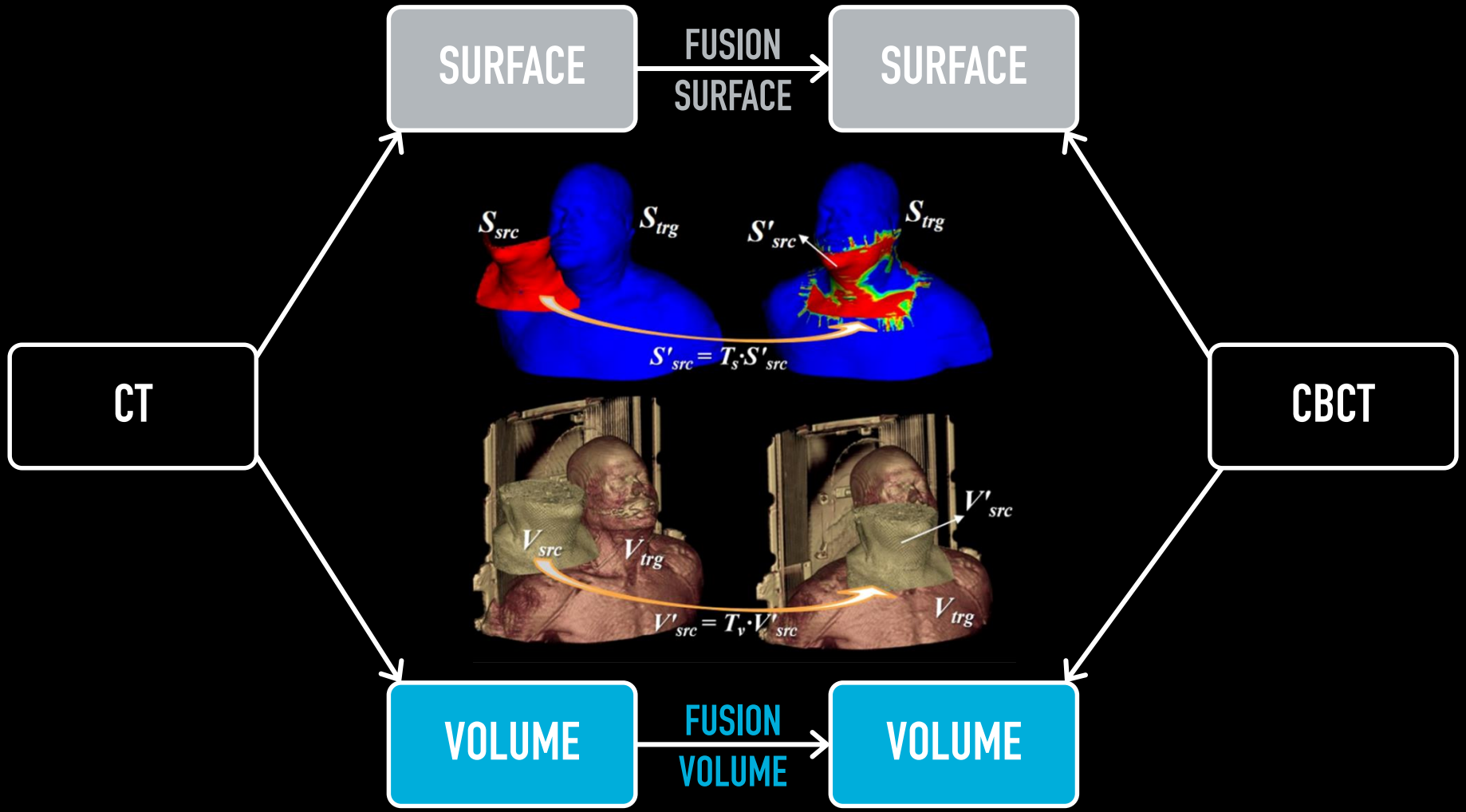

Kim, Y., Li, R., Na, Y. H., Lee, R. & Xing, L. Accuracy of surface registration compared to conventional volumetric registration in patient positioning for head-and-neck radiotherapy: A simulation study using patient data. Med. Phys. 41, 121701 (2014).

EXACTRAC PROPOSITION
SUPERIOR MONITORING ACCURACY

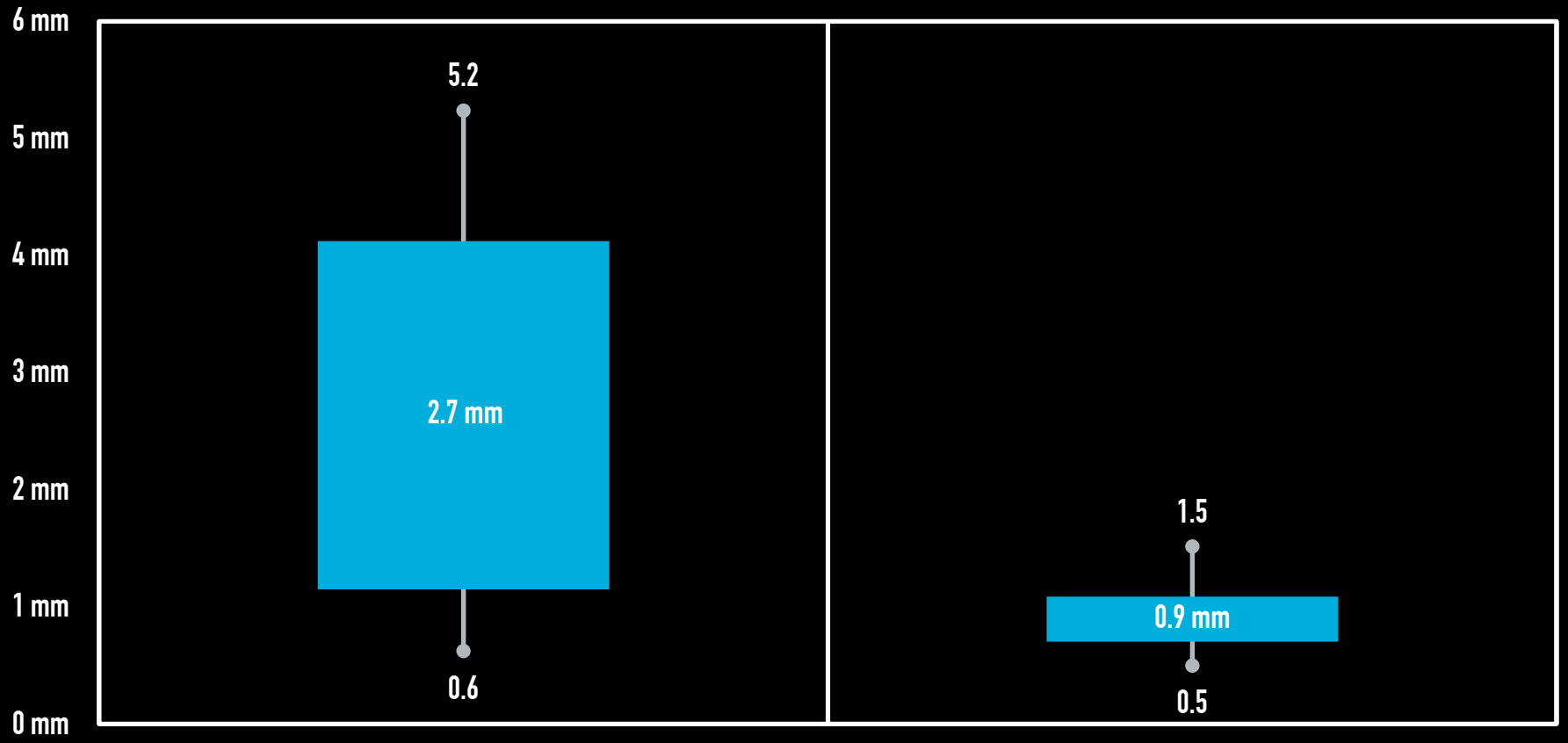

The mean and max total difference between both resulting transformation matrices underlying the respective fusions

Assessment of the accuracy of the iterative closest point (ICP) surface fusion algorithm by measuring the residual error

Kim, Y., Li, R., Na, Y. H., Lee, R. & Xing, L. Accuracy of surface registration compared to conventional volumetric registration in patient positioning for head-and-neck radiotherapy: A simulation study using patient data. Med. Phys. 41, 121701 (2014).

EXACTRAC
LINAC INDEPENDENT COMPATIBILITY

- Two kV-X-Ray units recessed in the floor
- Two flat panels
- Integrated optical tracking system
- Dual X-Ray generator
- Proprietary 6D fusion

State of the art Radiosurgery / IGRT system

Top Indications
- **Cranial**
- **Spine**
- **Lung**
- **Prostate**
- **Head and Neck**

VARIAN

900+ systems in 49 countries

180,000 fractions per month

ELEKTA

COMPATIBILITY WITH VARIAN PERFECTPITCH

- 6D positioning supported with ExacTrac 6.2

COMPATIBILITY WITH ELEKTA

- Seamless integration of ExacTrac with Elekta linacs
- Automatic loading of the patient treatment plan to ExacTrac from MOSAIQ®
- Patient positioning in 6 degrees of freedom with HexaPOD™ evo RT system

EXACTRAC
OPTIONS

FRAMELESS SRS
- Highly accurate delivery of single or multi-fraction SRS
- Rigid mask and fixation system

POSITION PACKAGES
- Automated patient positioning
- Range of platforms (BL Robotics, Hexapod, Perfect Pitch)

CBCT IMPORT AND ALIGMENT
Utilises CBCT data to allow soft tissue set up

IMPLANTED MARKER TRACKING
- Simple and automated approach to visualise and detect implanted markers
- Wide range of implanted markers supported

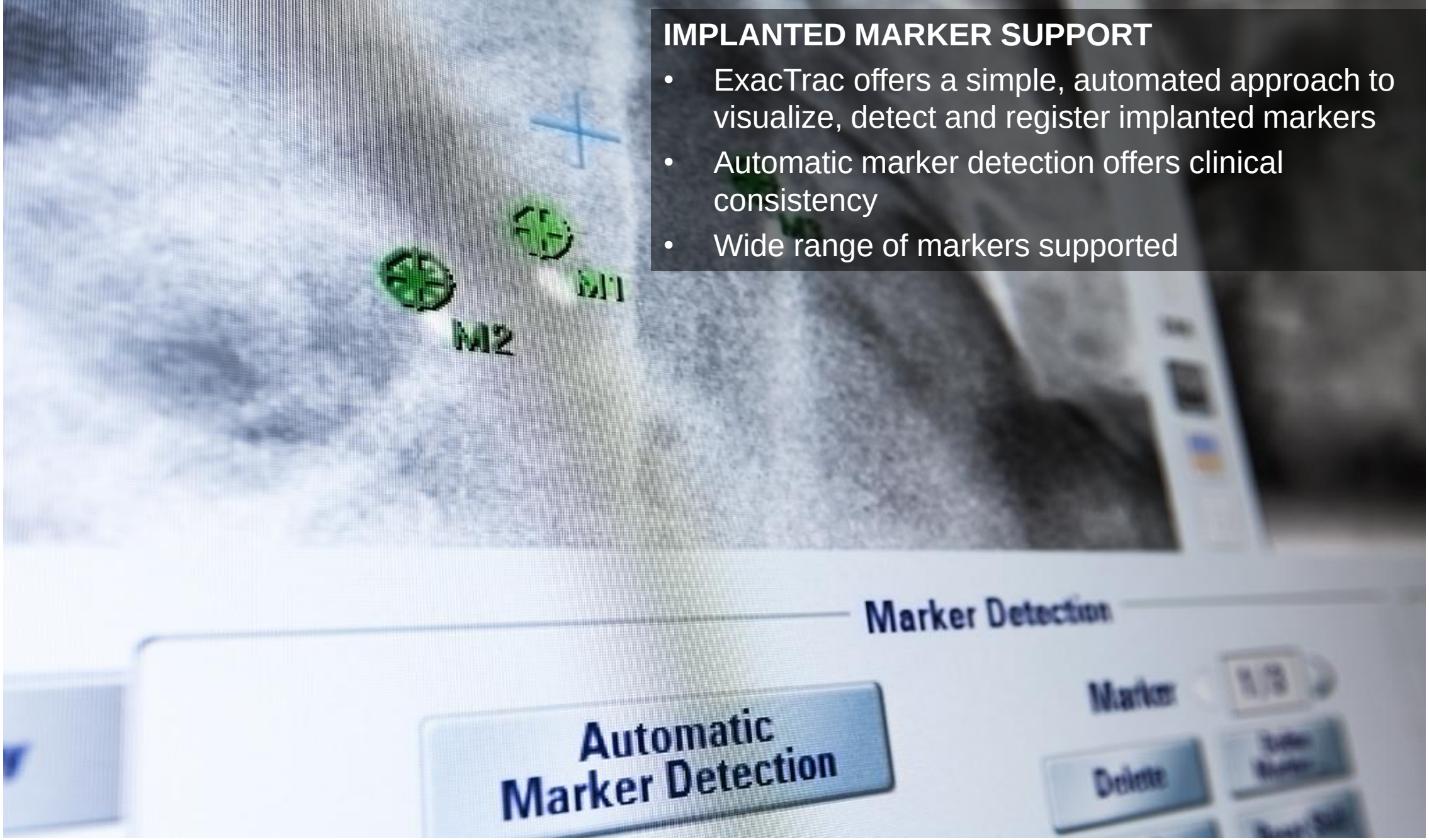

IMPLANTED MARKER SUPPORT

- ExacTrac offers a simple, automated approach to visualize, detect and register implanted markers
- Automatic marker detection offers clinical consistency
- Wide range of markers supported

FRAMELESS CRANIAL RADIOSURGERY

- Highly accurate delivery of single or multi-fraction treatment
- Precise non-invasive stereotactic mask system designed for re-producible conformity
- Streamlined workflow overcomes the restrictions of frame based radiosurgery

UNIQUE FEATURE: NON-COPLANAR VERIFICATION

- Intra-fractional motion management for linac based IGRT systems
- Continuous X-Ray verification throughout the entire treatment delivery, even at non-coplanar fields
- Gives confidence that the prescribed treatment has been delivered.

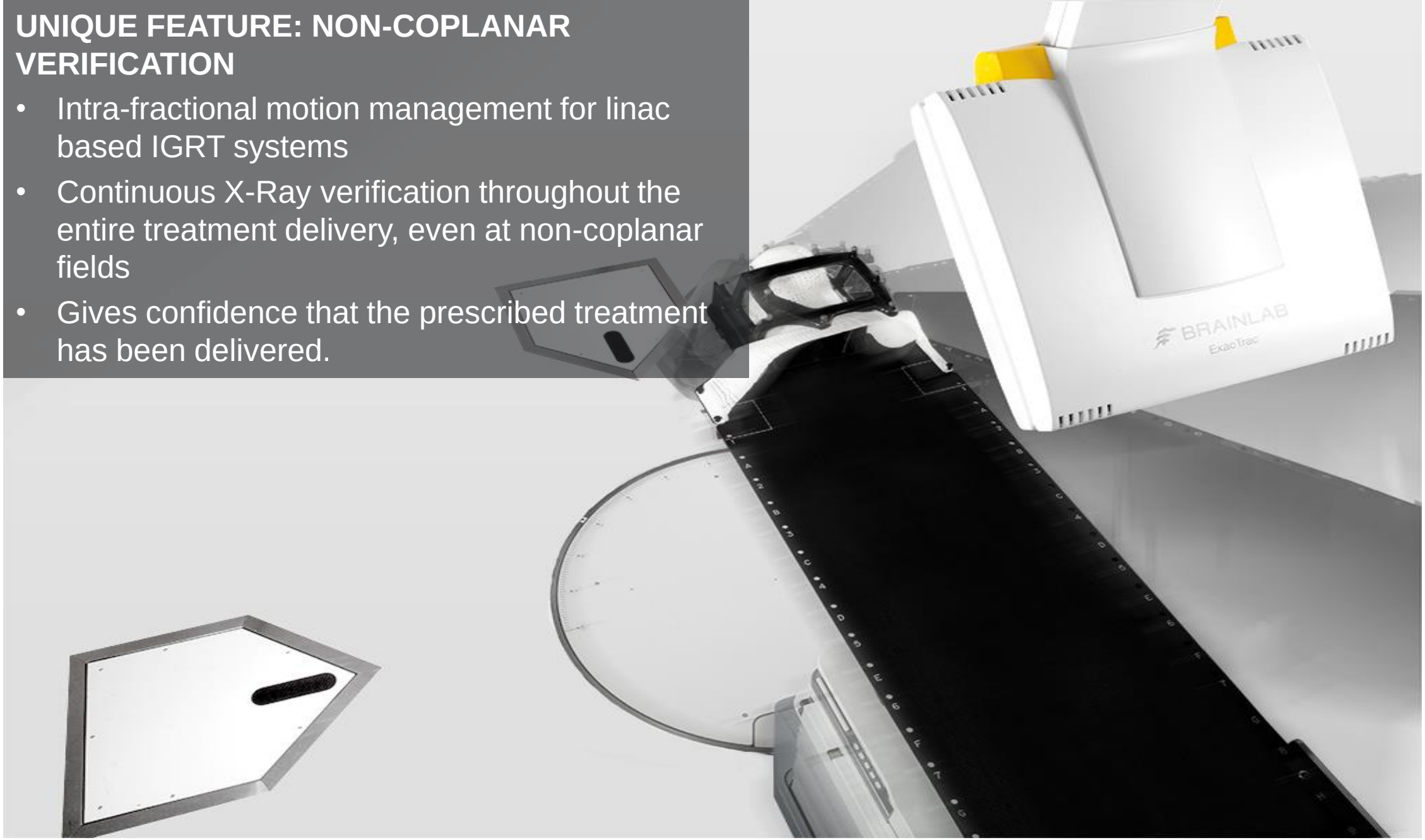

THANK YOU

pier.raguzzi@brainlab.com